ABSTRACT

BHAGWAT, SARANG SUNIL. An Environmental Life-Cycle Modeling and Analysis Framework for Microalgal Biofuels. (Under the direction of Dr. James W. Levis and Dr. S. Ranji Ranjthan.)

There is increasing interest in developing renewable alternatives to conventional fossil fuels. This is because the demand for transportation fuels is increasing, and fossil energy sources are finite as well as a leading source of greenhouse gas emissions. Microalgae-based biofuels present an alternative to crop-based biofuels with the potential for greater yields and reduced consumption of freshwater, fertilizers, and arable land; however, they are not currently a viable large-scale replacement due to the energy-intensive processes (e.g., drying) required to concentrate and convert the microalgal slurry into fuel. Recent and possible future advances in microalgal biofuel production technologies have the potential increase the cost- and energy-efficiency of microalgae-to-biofuel systems to make them competitive with conventional and crop-based transportation fuels.

Understanding the system-wide environmental implications of these new production pathways requires a systematic assessment of the entire microalgae-to-fuel system. The environmental impacts reported by life-cycle studies of algal biofuels are significantly variable and difficult to compare. This is chiefly because: 1) they extrapolated from bench-scale data; 2) they used simplistic models to estimate algae productivity; or 3) they used inconsistent system boundaries. There are frameworks that use more detailed models such as the Biomass Assessment Tool (BAT), the Algae Logistics Model (ALM), or the Algae Farm Cost Model, but they are not available for outside use and the data and calculations they use are not readily accessible to review or update. Studies on individual algal biofuel production technologies are often limited by the lack of a framework that would enable them to quickly assess the system-wide implications of their research.

To address these limitations, we developed an open-source framework for systematically modeling and evaluating location-specific production and use of algal biofuels that integrates dynamic process models throughout the production chain from cultivation through fuel production and use. The environmental and energetic impacts associated with six biofuel production-and-use pathways, constructed using models of relevant technological alternatives,

were assessed and compared with those of conventional low-sulfur diesel and soybean-based biodiesel. Sensitivity analyses were conducted to characterize the influence of process parameters on life-cycle environmental and energetic performance of the biofuels. The results indicate that, with certain system improvements and optimization, microalgae-based biofuels may environmentally outperform conventional diesel and compete with soybean-based biodiesel using existing technologies. While variable productivity estimates used by previous life-cycle studies (ranging from 3 to 96 $g.m^{-2}.d^{-1}$) is reported as a notable source of variability in life-cycle impacts for lower productivity, significantly increasing the PBR biomass productivity beyond approximately 15 to 20 $g.m^{-2}.d^{-1}$ had a relatively minor effect on energetic and environmental performance. The source of electricity consumed on-site significantly affected the results; switching from 100% fossil marginal grid mix to a potential 0% fossil electricity improved the greenhouse gas performance of illustrative algal biofuel production chains by approximately 26 to 140 g CO_2 eq. MJ^{-1} (58 to 84%) The modeling-and-analysis framework developed is capable of integrating future technologies into life-cycle assessments of full microalgae-to-biofuel systems and making recommendations for targeted improvements in production chains. The framework can also be extended and applied to other fuels to improve understanding of their energetic and environmental performance.

An Environmental Life-Cycle Modeling and Analysis Framework for Microalgal Biofuels

by
Sarang Sunil Bhagwat

A thesis submitted to the Graduate Faculty of
North Carolina State University
in partial fulfillment of the
requirements for the degree of
Master of Science

Environmental Engineering

Raleigh, North Carolina
2019

APPROVED BY:

_____	_____
James W. Levis Committee Co-Chair	S. Ranji Ranjithan Committee Co-Chair
_____	_____
Joel J. Ducoste	Francis L. de los Reyes III

DEDICATION

The work presented herein is dedicated to my late mother, Dr. Mahalaxmi S. Bhagwat.

BIOGRAPHY

Sarang Bhagwat received his Bachelor's in the Technology of Oils, Oleochemicals, and Surfactants from the Institute of Chemical Technology, Mumbai in 2017. He began his Master's in Environmental Engineering at North Carolina State University, Raleigh in the Fall 2017 semester. From Summer 2018 – Summer 2019, he worked on two research projects: the first, under the advisement of Dr. J. W. Levis, involved modeling the kinetics of the disinfection of industrial wastewater, and subsequently analyzing the life-cycle implications of various disinfection strategies; the second, involving life-cycle modeling and analysis of microalgae-to-fuel systems under the advisement of Dr. J. W. Levis and Dr. S. R. Ranjithan, is described in this thesis.

ACKNOWLEDGMENTS

The author would like to note the contributions of the following people:

- His advisors, Dr. J. W. Levis and Dr. S. R. Ranjithan, who guided him throughout this project;
- The National Science Foundation, for funding the research presented herein;
- His professors at the Institute of Chemical Technology, Mumbai as well as North Carolina State University, Raleigh, whose tutelage gave him the tools necessary to perform scientific discovery and reasoning;
- His parents (Dr. Sunil S. Bhagwat and Mrs. Meghana S. Bhagwat) and his grandparents (Dr. Geeta S. Bhagwat and Dr. Subhash S. Bhagwat), along with the rest of his family, whose steadfast support counted for perhaps the most.

TABLE OF CONTENTS

LIST OF TABLES

LIST OF FIGURES

CHAPTER 1. INTRODUCTION

There is increasing interest in developing renewable alternatives to conventional fossil fuels. Fossil energy sources are finite and demand for them is increasing; for example, the International Energy Agency has projected global energy demand to increase by 27% between 2017 and 2040 [1], and the US Energy Information Administration estimates that US energy demand for transportation will increase by almost 45% in this time [2]. Currently, the predicted costs of advanced biofuels are highly uncertain and generally uncompetitive with fossil fuels [3][4]. However, technological advances have the potential to reduce biofuel costs, while the price of crude oil is projected to more than double from 52 $/barrel in 2017 to 108 $/barrel by 2050 [5].

Microalgae have been suggested as a promising source of renewable, low-impact transportation fuels [6][7][3]. Unlike soybean- or corn-based biofuels, microalgal biofuels can avoid competition with food by being grown on less and non-arable land with brackish/lower-quality water, wastewater, or sea water [7]. Other advantages include higher annual yield per hectare of land [3][8][9], year-round cultivation in appropriate climates or with supplemental heating and cooling [7], significantly higher concentrations of lipids and carbohydrates [9].

Given the wide-ranging impacts of large-scale fuel production, it is important to consider the adverse environmental impacts associated with microalgal biofuel production and consumption (e.g., global warming potential, air pollution, energy use, and water use) as compared to conventional fuels. Often, rather than implementing full production chains to assess the state of production performance, efforts to make microalgal biofuels commercially and environmentally viable focus on developing and optimizing the individual processes associated with the generation of microalgal feedstock through to the production of fuel [3][8]. Using data and models for all such processes involved, system-wide environmental life-cycle assessments (LCAs) may be performed. Environmental LCA is a systematic framework for evaluating the environmental emissions and impacts associated with systems (such as for biofuel production) as well as the processes they are comprised of.

LCA can be used to compare alternative processes in microalgae-to-fuel systems, to identify critical processes, and to compare microalgae-based fuels to other biofuels and conventional fuels. Existing life-cycle tools and analyses have led to widely disparate estimates of the greenhouse gas (GHG) emissions and net energy production from microalgae-to-biofuel systems [3][8][10]. For example, a review by Quinn et al. [3] reported that published well-to-pump GHG emissions from microalgae-based fuels using photobioreactors (PBRs) range from -75.29 [11] to +195 g CO_2 eq./MJ eq. [12]. Estimates of algal biomass productivity in particular have been a major source of uncertainty with published ranges from 3 to 96 $g.m^{-2}.d^{-1}$ being used [10][11][8][13]. There is significant variability in the complexity of models used to estimate annual biomass and lipid yields. Quinn et al. [3] report that the use of productivity models that do not consider the influence of temporal variations in temperature and other weather parameters have led to unrealistic extrapolation of laboratory data. The same paper also says that dynamic seasonal modeling of algal growth is "an important next step in scalability assessments" [3].

The growth of microalgae is dependent on temperature and the availability of photosynthetically active radiation (PAR). The temperature in the reactor and the PAR reaching the algae are dependent on several meteorological parameters (e.g., global horizontal irradiance, air temperature and pressure, wind velocity, and relative humidity) at the chosen location as well as the configuration of the cultivation system. Potential configurations include open raceway ponds and bubble-column, tubular, and flat-plate PBRs [7][14].

Many studies have found that algae dewatering and drying are typically the largest contributors to global warming potential and cumulative energy demand [8][15][12][3]. Research focused on fuel conversion technologies that reduce or eliminate the need for drying (e.g., hydrothermal liquefaction, pyrolysis, and supercritical methanolysis) has offered processes that have the potential to perform better environmentally in a full production chain [16][17][18]. Existing process models can estimate fuel yield and properties based on composition of input biomass, and the developers of these models frequently recommend integrating these models with those of upstream processes and biocrude post-processing in future life-cycle studies [16][19]. Likewise, there are dynamic algae PBR cultivation models that have been validated against industrial-scale flat-plate PBRs and can be integrated into LCAs of microalgal biofuels [14][7]. Data is also available for emissions from the combustion of various biofuels based on their feedstock and

production pathway, such as Argonne National Laboratory's GREET [20][21]. These existing models and data provide a foundation for the development of a life-cycle framework capable of assessing entire fuel production chains and use.

Frameworks using models that address spatiotemporal variability in production parameters, such as the Biomass Assessment Tool (BAT) [22], the Algae Logistics Model (ALM) [23], or the Algae Farm Cost Model [24] are not available for public use. Studies on individual algal biofuel production technologies [16][19] are often limited by the lack of a framework that would enable them to quickly assess the system-wide implications of their research. There is a need for an openly available life-cycle tool that provides a framework to easily and meaningfully integrate advancements in algal biofuels research, evaluate the environmental emissions, resource use, and impacts associated with alternative algae-to-fuel production chains, and compare their performance to conventional fuels and crop-based biofuels.

The objective of this study is to develop and present an open-source life-cycle framework capable of (i) estimating the emissions, mass and energy flows, and impacts associated with the production and use of biofuels from microalgae for a given location and process chain with user-defined system boundaries; and (ii) identifying the critical model parameters and processes that have the greatest influence on environmental performance, thus highlighting areas for further research and development.

The overall modeling framework and the process models are described in Chapters 2 and 3 respectively. Chapter 4 describes the configuration of the analysis conducted in this including the illustrative scenarios that were compared, and this is followed by a presentation and discussion of the results in Chapter 5. Several limitations and other considerations before use of the framework are discussed in Chapter 6. Concluding remarks and implications of this study are discussed in Chapter 7.

CHAPTER 2. MODELING FRAMEWORK

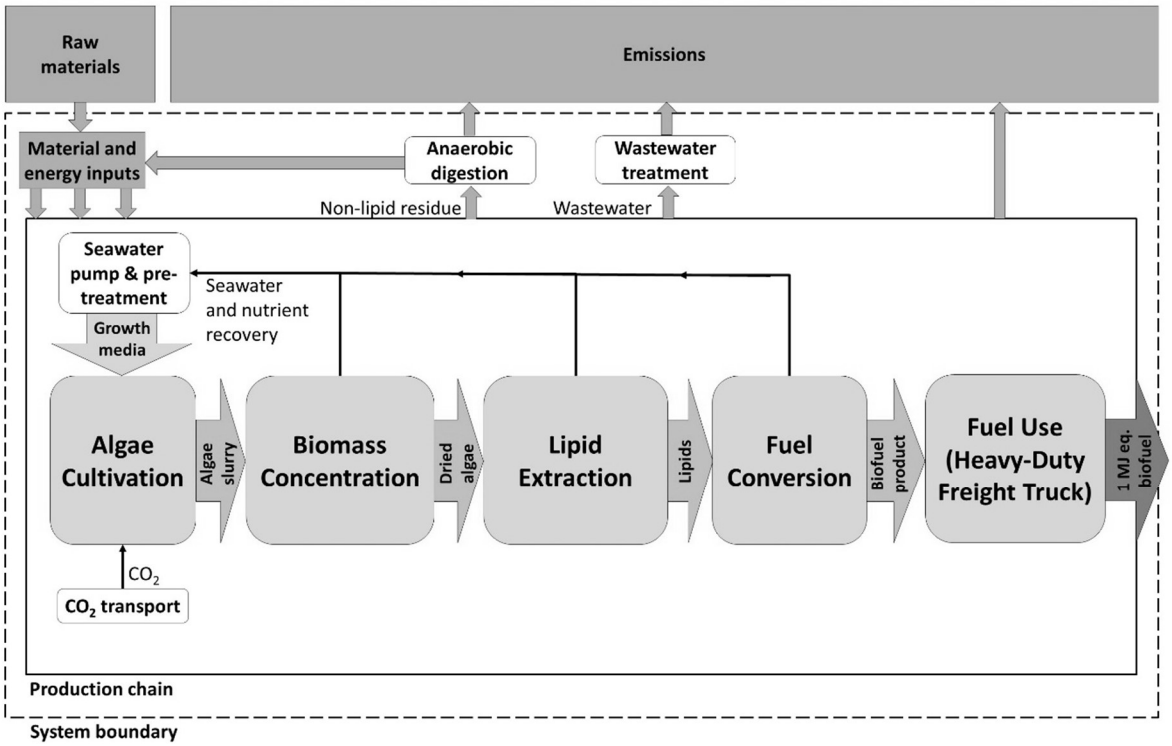

Figure 1. Mass flow through a typical algal biofuel production-and-use-chain.

This study presents a life-cycle modeling framework to construct and analyze location-specific biofuel production-and-use chains. Figure 1 illustrates a typical chain that begins with the production of feedstock biomass, followed by processes to prepare this biomass for the selected conversion technology; e.g. by concentrating an algal slurry (using harvesting, dewatering, and drying technologies) and/or extracting specific components from the biomass (such as hexane-based extraction of lipids). Impacts from the anaerobic digestion of residual biomass (for residue composition for which literature describes this as feasible) and treatment of effluent wastewater are also considered. Stabilization and hydroprocessing of biocrude for use in automobiles may be necessary based on conversion output properties. Vehicle-specific combustion is modeled based on calculated biofuel composition, and parameters from GREET [20] for equivalent performance of other fuels are used by scaling emissions to mass combusted.

For each process shown in Figure 1, life-cycle inventory models that estimate process requirements (material and energy) and output properties were developed for selected default

technology alternatives. The default data and equations used in these models were adapted from existing peer-reviewed academic literature and government reports on microalgal fuel production.

Multiple criteria were used to determine the data and equations to be used in the default process models. All of the included studies provided data from industrial-scale operations or were validated against industrial-scale facilities. Priority was given to studies that focused on algal biomass feedstocks, and the only process that used data not associated with algae was methyl esterification of lipids, which was based on soybean lipids. Level of modeling detail was prioritized next (e.g., for HTL, the models from Leow et al. [19] which calculate fuel yield and composition based on input biomass composition were preferred over the static yield and composition estimates in Bennion et al. [8]). Recency of the studies was prioritized next, and US-located studies were prioritized over those conducted internationally. Lastly, the National Alliance for Advanced Biofuels and Bioproducts (NAABB) final report [17] was also generally prioritized over other studies with all other criteria being equally satisfied.

In constructing a microalgal biofuel production chain, the user may select from among the technology alternatives included for each process, provided the input requirements of each successive step are satisfied. The user may also specify the regional weather data from the National Solar Research Database (NSRDB) that is to be read. Several process-specific parameters and decisions are also configurable, such as burning the by-products from pyrolytic conversion to alleviate heat requirement or actively maintaining broth temperature during algae cultivation within an optimal range to facilitate growth.

2.1. Functional Unit and System Boundary

The functional unit used in the model can be specified by the user. Available options include units based on: (i) the mass of fuel produced; (ii) the energy content of the produced fuel; (iii) tonne-km of freight transport using the fuel. The system boundary can also be adjusted to only consider process chains up to fuel distribution (well-to-pump) or through fuel combustion in vehicles (well-to-wheel). The analysis configuration used in this study is described in Section 4.

2.2. Environmental Impact Parameters

In life-cycle impact assessment (LCIA), for each category of impact considered, databases are used with factors assigned to each inventory and environmental flow. These factors characterize impact relative to that of a specific flow (usually one that is commonly associated with said impact). Table 1 shows the selected life-cycle impact indicators and methodologies considered by the framework.

Impact categories were included based on their relevance to the production and use of conventional and renewable fuels. Global warming potential (GWP) was selected based on the prominent carbon flows throughout the system (e.g. in CO_2 capture, biomass anaerobic digestion, and fuel combustion). IPCC 2007 was selected over later methodologies per the US Environmental Protection Agency's recommendation [27]. It is necessary to track cumulative energy demand from fossil fuels to ascertain if the algae-based biofuel system produces more or less energy than it utilizes (including energy required to produce the system's material inputs), which is a measure of its long-term sustainability. Eutrophication and acidification are significant given the use of fertilizers as sources of nitrogen while cultivating algae and other biofuel feedstocks. Nitrogen oxides (NO_x), which contribute to smog formation, are emitted when fuels are combusted. TRACI ascribes photochemical oxidation impacts to various flows as equivalents of mass NO_x. While land use could be considered as a significant impact in renewable liquid fuel production, available information was insufficient for the footprints of the various technologies considered by this study to make a fair comparison. Finally, freshwater use was included as an impact, since soybean-based biofuels have been criticized as freshwater-depleting and algal biofuels have been reported to perform better in this regard [7].

Table 1. Environmental impacts and their associated methodologies as implemented in the framework.

Parameter	Unit	Methodology	Reference
Global Warming Potential – 100 annum (GWP-100a)	g CO_2 eq.	IPCC 2007	[25]
Cumulative Energy Demand – Fossil Fuels (CED-f)	MJ eq.	Ecoinvent v3.2	[28]
Freshwater Use	L	Ecoinvent v3.2	
Eutrophication	mg N eq.	TRACI	[26]
Photochemical Oxidation	mg NO_x eq.	TRACI	
Acidification	mmol H^+ eq.	TRACI	

2.3. System Model

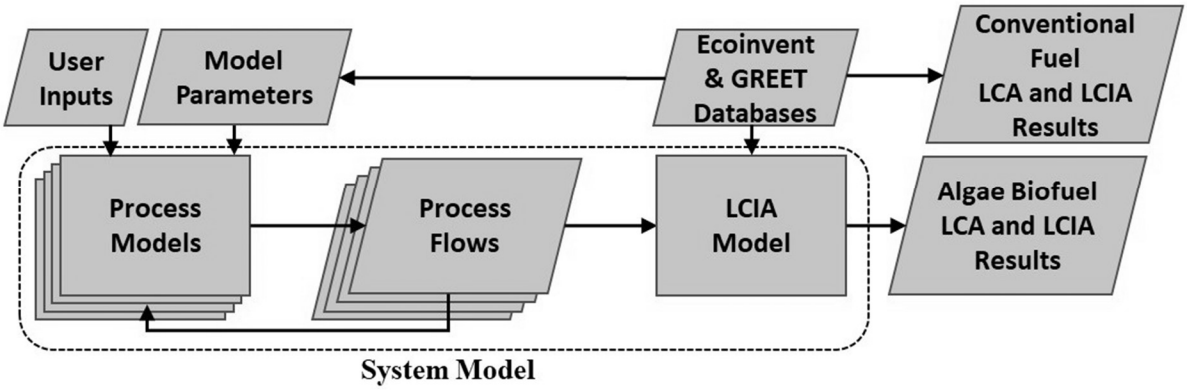

Figure 2. Flow of data through the system model.

The model for algae cultivation in PBRs developed by Quinn et al. [14] provided a starting place for the overall framework developed here. As it estimates the biomass output and concentration as well as composition as lipids, carbohydrates, proteins, carbon content, and nitrogen content, it made sense to develop downstream models that integrated these data in their calculations. Using parameters sourced from existing literature, we created process models in *Python* for several alternative technologies used in the processes described in Figure 1. Material, energy, and input composition requirements, direct emissions, and output properties are calculated in each model. Descriptions of each process model can be found in Section 3.

A user can combine the process technology choices to define a biofuel production-and-use chain by specifying inputs that include location, technologies used, supplemental heating and cooling of PBR, handling of co-products, analysis boundary, and functional unit. The framework reads weather data directly as a comma-separated file downloaded from NSRDB. The scenario construction code calls models of each selected technology as instances. As illustrated in Figure 2, successive instances receive data on the flow of mass from previous instances and ascertain that input criteria are met, following which material and energy requirements, direct emissions, and mass output flow properties are estimated and stored to a dictionary to be referenced by the next instance.

The functional quantity of fuel produced is then calculated based on the final process model instance's output properties and the analysis configuration specified by the user (e.g., a mass of 450 kg biodiesel times a higher heating value of 39.8 MJ/kg biodiesel for a functional quantity of 17910 MJ eq. of biodiesel, when the user specifies a functional unit of 1 MJ eq. within a well-to-wheel boundary). Then, a vector comprised of material and energy requirements and direct emissions for each process model instance is multiplied by a matrix comprised of the impact factors assigned to each of these inventory flows by Ecoinvent v3.2 to estimate the impacts (Table 1) of each process. Each impact is divided by the functional quantity to represent impacts on a functional unit basis (e.g. GWP in g CO_2 eq. / MJ eq.). This enables an analysis of the impact contributions of each process and each inventory flow, and comparisons of the net impacts of multiple constructed scenarios mutually and with data from GREET and Ecoinvent v3.2 for conventional fuels.

The models currently implemented in the framework only estimate operational requirements of material and energy, and do not consider requirements during construction and installation.

2.4. Sensitivity Analysis

For each constructed production-and-use chain (Section 4.3), a Monte Carlo simulation was conducted. The parameters of all process models were simultaneously and randomly varied within reported uniform, triangular, and log-normal distributions. Estimates of the dependent impacts were recorded for each of 8,000 iterations. The correlation between each impact and

parameter was quantified using Spearman correlation coefficients in *MS Excel*. This enabled us to identify the parameters most influential to each impact in the production-and-use chain. These influential parameters were then singly varied to track their independent effects on the impacts.

Initially, the study also intended to include uncertainty shown as error bars for each estimated impact. Latin hypercube sampling was initially considered to ensure the full breadth of parameter distributions was adequately represented, but it was found that 8,000 iterations using purely random sampling based on reported distributions was adequate for the standard deviation and mean output to converge. However, the unavailability of reported statistical distributions for several parameters meant that generic distributions had to be used for several parameters, and it was decided against proceeding with that portion of the analysis for fairness of comparison.

CHAPTER 3. PROCESS MODELING

Life-cycle inventory models were developed using Python 3.7 for each of the processes shown in Figure 1. In addition to tracking the properties of mass throughput, the models estimate the emissions and fuel, energy, and material use associated with each process alternative. Each successive model imposes requirements based on input parameters (e.g. biomass concentration), which are tracked throughout the production chain. The criteria used for the inclusion of data from literature references to the implemented process models are discussed in Chapter 2. The models currently implemented in the framework only estimate operational requirements of material and energy, and do not consider requirements during facility construction and equipment installation.

3.1. Procurement and Handling of Seawater and CO_2

Seawater and CO_2 are the primary material inputs for algae cultivations. For use as growth media, seawater must initially be treated to minimize presence of microbes. This treatment is modeled using data from Al-Sarkal et al. [29] for pre-treatment of seawater in desalination plants via ultrafiltration.

CO_2 is chemically adsorbed on a solvent (e.g., an amine) and then regenerated via thermal induced desorption [20]. The energetics for capture of CO_2 and transport through pressurized pipeline are both modeled using parameters from GREET. The captured CO_2 is sparged continuously through all operational PBRs at 2.5 L of CO_2-enriched air per liter of culture per minute (or VVM) [14]. The CO_2 requirement is dictated by carbon content of biomass produced annually as estimated by the cultivation model.

3.2. Cultivation in a Flat-Plate PBR

The cultivation process model estimates the annual algae production and composition along with the associated fuel, electricity, and material use. The pre-treated seawater is enriched with nitrogen and phosphorus using urea and diammonium phosphate.

The model described by Quinn et al. [14] was adapted for this study. It simulates microalgae growth and lipid accumulation in an outdoor, industrial-scale, flat-plate photobioreactor (PBR) and considers local weather (e.g., solar radiation and temperature), microalgae species, and reactor geometry [14]. Half-hour time steps are used to model growth over the course of the year using weather data from the National Solar Radiation Database [30]. Algae are harvested when a set concentration is reached (e.g., 3 g/L). The model uses a carbon-specific growth rate as a function of the photosynthetic rate, the specific uptake rate of nitrogen, and the maintenance respiration rate. The dependencies of these rates on temperature and light distribution are also incorporated.

PBR reactor temperature is also modeled at half-hour time steps using location-specific values for air temperature, air pressure, global horizontal irradiance, wind velocity, and relative humidity. PBR temperature is calculated at each step as a function of the enthalpies of evaporation, convection, solar radiation, and the Stefan-Boltzmann radiations of air and water. The effect of temperature on microalgae growth is characterized using a temperature efficiency factor, which is modeled as a bell curve centered around the optimal growth temperature (e.g., 23°C for *Nannochloropsis oculata* [14]) based on the model developed by Alexandrov and Yamagata [14] [31].

In addition to using a temperature efficiency factor, our model conservatively assumes that the entire culture is reset to initial concentration and composition if the reactor operates outside a temperature range of 5 to 40 °C for *N. oculata*; this range was assumed based on a literature survey. Bechet et al. [32] reports a lethal temperature of 43°C for *D. salina*, a species of seawater algae, with complete loss of viability and photosynthetic activity at this temperature. According to Sukenik et al. [33] the repair process for *Nannochloropsis* struggles to keep up with the thermally induced damage past 32 °C. Additionally, Bae et al. [34] observed that at 10°C, the growth rate of *N. oculata* was among the lowest observed among several species of *Chlorella*, *Nannochloris*, and *Nannochloropsis*. However, a lower survivable temperature was assumed for our model, based on Ras et al.'s [35] observation of less abrupt effects of temperatures decreasing below survivable range compared to those exceeding it. Optional electrical heating and cooling is also modeled to maintain reactor temperature close to optimum or within a user-specified range.

Light dependency is modeled by calculating photosynthetic rate as a function of light intensity. Light distribution is currently modeled using the average 1st-order Beer-Lambert light intensity throughout the reactor and depends on biomass concentration as well as reactor dimensions [14]. Annual solar data in half-hour increments from the selected location are read directly by the cultivation model, and discrete results for energy use (pumping for harvest, steady mixing and sparging of CO_2-enriched air, and optional heating or cooling), biomass concentration, and biomass composition may also be plotted along this timeline.

The default parameter values used in the flat-plate PBR growth model are shown in Table A-1.

3.3. Algae Concentration

The biomass-enriched medium output by the cultivation process is concentrated in one or more distinct steps. An initial harvesting step may be followed by a dewatering step and supplemented by a more intensive drying step, depending on input requirements of the lipid extraction and fuel conversion processes. The default biomass loading concentration is 3 g/L or about 0.29 % w/w (concentration of output from PBR by Quinn et al. 2011 [14]), and it is important to ensure this falls within the input requirements of any technology employed for harvesting. An output concentration of 8 to 10 % w/w is typical for this process, although technologies that further concentrate the output may be employed as single-step harvesting and dewatering processes. Available options for harvesting technologies are listed in Table 2.

Table 2. Reported performance parameters of harvesting technology alternatives modeled.

Harvesting technology	**Electricity requirement**	**Minimum incoming solids content (% w/w)**	**Maximum achievable solids content (% w/w)**	**Biomass recovery (%)**	**Reference(s)**
Electroflocculation + DAF	0.1553 kWh / m^3 throughput	0.05	2.94 – 3.92 (30 – 40 g/L)	87	[36]
Electrocoagulation	0.026 kWh/kg algae	0.02	8	98	[18]
Pressure Filter (Netzsch Chamber Filter)	0.88 kWh / m^3 throughput	0.05	22 – 27	98	[37] [38]
Vacuum Drum Filter (Dorr Oliver)	5.9 kWh / m^3 throughput	0.05	18	98 (assumed)	[37] [38]

While the Netzsch chamber pressure filter can act as a single-step harvesting and dewatering process and has relatively low electrical consumption, Pahl et al. [38] noted that it is a discontinuous process (unlike the belt press filter and vacuum filter) due to the method used for recovering the biomass cake. They also report that while some operational automation is possible, the technology is seldom used for microalgae dewatering.

Filtration technologies are reported to be susceptible to fouling and clogging regardless of the driving force (pressure-driven or vacuum-driven)[39]. Fasaei et al. [39] has noted the high operational cost of vacuum filtration relative to its pressure-driven counterpart technologies (Netzsch chamber pressure filter, Bellmer belt press filter). Molina Grima et al. [37] and Pahl et al. [38] both reported the Dorr Oliver vacuum drum filter as unreliable and the Netzsch chamber pressure filter as highly reliable for this application. It is important to note that the use of polymers to facilitate floc formation prior to pressure-driven filtration is not included in the process models.

During electrocoagulation, the electrodes (stainless steel 316 plates) deplete and must be routinely replaced. The rate of replacement was modeled using stainless steel 316 plate life replacement cost in USD/m^3 slurry throughput reported by Richardson et al. [18] and average USD price per kg of stainless steel 316 [40]. Depletion of aluminum electrodes during the combined electroflocculation + DAF process was modeled using data from Shi et al. [41].

After a harvesting process concentrates the slurry typically to 8 to 10 % w/w, the slurry often needs to be further concentrated to between 80 and 100 % w/w depending on the methods used for lipid extraction and fuel conversion. There is often an initial dewatering step to increase the solids content to about 15 to 20 % w/w, which is followed by a more energy-intensive drying step that evaporates excess moisture to reach the final solids content desired prior to fuel conversion (which is the lesser of [i] the default concentration output by the drying process and [ii] the required threshold value specified by the conversion process). The key variables associated with dewatering and drying processes include the minimum incoming solid content, expected achievable solids content, and electricity and fuel use per unit mass of water throughput or water removed. Common dewatering options include belt presses, centrifuges, spiral plate rotors, and filters, while common drying options include direct thermal drying, spray drying, methane-fueled drums, and heat-integrated dryers. Default input values for the modeled dewatering and drying options are shown in Tables 3 and 4, respectively.

Table 3. Reported performance parameters of the dewatering technology alternatives modeled.

Dewatering technology	**Electricity requirement (kWh/m^3 throughput)**	**Minimum incoming solids content (% w/w)**	**Maximum achievable solids content (% w/w)**	**Biomass recovery (%)**	**Reference(s)**
Belt Press Filter (Bellmer)	0.5	4.0	18	98% (assumed)	[37] [38]
Disc-Stack Centrifuge	0.7 – 1.3	0.05	15 – 20	95 – 99	[39] [42]
Spiral Plate Rotor Centrifuge	0.95 – 2.00	0.05	20 – 22	95 – 99	[39]

Table 4. Reported performance parameters of the drying technology alternatives modeled.

Drying technology	**Heat requirement (MJ/kgH_2O removed)**	**Maximum achievable solids content (% w/w)**	**Biomass recovery (%)**	**Reference(s)**
Direct Thermal Drying (gas-fired dryer)	3.556	90	100	[43]
Spray Dryer	3.3 – 3.9	90 – 95	99	[39] [42]
Drying Drum	3.24	90 – 95	99	[39] [42]
Heat-Integrated Dryer (Delft)	2.02	90 (assumed)	99 (assumed)	[42]

Any of the listed dewatering processes with a suitably low minimum incoming solids concentration may be used for exclusively dewatering or as a single-step harvesting and dewatering process. As such any of the harvesting and dewatering technologies can be used in a

succession of increasing reported output concentration; the distinction made by this study between harvesting and dewatering is only related to the order (and consequently the output concentration) of the process. Additionally, it is important to note that the use of polymers to facilitate floc formation prior to pressure-driven filtration is not included in the process models.

Pahl et al. [38] noted that centrifugation generally involves high capital and operational expenses, and that this must be considered in conjunction with its reputation as a reliable dewatering technology. It has been reported by Pahl et al. [38] that the issue of centrifugation process liquid (used to aid in discharge of residual solid matter) diluting the output has been addressed by a new 'Spiral Plate Technology' from Evodos^{TM} that allows particles to settle faster.

The subsequent drying step is reported to generally consume the most electricity of all the production processes [38][3][42]. Direct heating is considered too energy-intensive for this application [38], although at the smallest scale this technology may be the optimal choice due to its potential for minimizing capital investment [42]. Spray drying is typically preferred at large production facilities because it is more cost-effective than other methods at large scales [39], but use of a drying drum is more energy efficient [39]. The prototype heat-integrated dryer developed at Delft University reportedly reduces heat requirements by almost 38% compared to using a drying drum [42].

A drawback common among the default process models for algae harvesting, dewatering, and drying is that while all are provided with reported or generic distributions for recovery rates and energy use, the two parameters are not coupled (e.g. higher electricity use for higher recovery rates).

3.4. Lipid Extraction

The lipid portion of biomass contains most of its energy content. Certain conversion processes (e.g. methyl esterification) require lipids to be separated from algal biomass. This is typically done using a solvent that can dissolve lipids (e.g. hexane). The default parameter values for lipid extraction process models are shown in Table A-2.

3.4.1. Conventional Dry Hexane Extraction

Hexane, an organic solvent, is used to separate the lipid fraction from the rest of the algal biomass. Electricity use, heat use, and hexane loss were regressed to the output lipid mass in the mass and energy balance data for hexane-based extraction of lipids from microalgal biomass reported in Hou et al. [44]. Multiplying the lipid recovery ratio (based on typical soybean lipid content) by the lipid content of throughput biomass, the mass of extracted lipids was calculated. Tap water use was calculated per unit throughput biomass from the reported values for soybean oil extraction in Cheng et al. [45].

3.4.2. Wet Hexane Extraction

A multi-stage process for extraction of lipids directly from a 10-20% w/w algal slurry has been developed by Valicor Renewables and assessed by the National Alliance for Advanced Biofuels and Bioproducts (NAABB) [17]. A pre-treatment stage in Valicor's trademark process reportedly includes flocculation and belt-press drying; however, the compound used as flocculant was not revealed by the company [9].

The material and energy requirements as well as lipid yield were adapted from Gehrer et al. [9]. A similar wet hexane extraction procedure discussed by Sathish et al. [46] added sulfuric acid to the slurry to cause precipitation of biomass prior to adding hexane; the quantity reported by Gehrer et al.'s [9] as "unspecified chemical" in the 'AlgaFrac' process will therefore be characterized as reagent-grade sulfuric acid in our study.

3.5. Fuel Conversion

The conversion of algal slurry to transportation biofuel must produce a fuel with a higher heating value similar to conventional diesel and have combustion properties that allow use in a conventional diesel engine, like a compression-ignition direct-injection (CIDI) engine. Models for four such processes are included in our framework. Calculations and/or values for higher heating values (HHVs) for fuels produced via each process modeled are shown in Table 5. The two thermochemical processes included – namely pyrolytic conversion and hydrothermal liquefaction – produce bio-oil that needs further processing (Section 3.6) before use as

transportation fuel [8], and it is assumed that bio-oil HHV does not change significantly during these processes since nothing in the literature was found to indicate otherwise. The default parameter values for fuel conversion process models are shown in Table A-3.

Table 5. Higher heating values for the products of the four conversion processes listed.

Conversion process	**Higher heating value (MJ/kg)**	**Reference(s)**
Methyl esterification	$= \sum_{i=1}^{\infty}(46.19 - \frac{1794}{M_i}\ 0.21 * N_i)$ where M_i is the molecular mass of and N_i is the number of double bonds in the *i*th fatty acid methyl ester. (39.8 for *N. oculata*.)	[47] [48]
Supercritical methanolysis	42.0 (reportedly 41 - 43)	[17]
Pyrolytic conversion	36.0	[17]
Hydrothermal liquefaction	$= 0.338 * C\% + 1.428 * \left(H\% - \left(\frac{O\%}{8}\right)\right) + 0.095 * S\%$ where C%, H%, O%, and S% are respectively the percent mass of bio-oil as carbon, hydrogen, oxygen, and sulfur respectively. (38.9 for *N. oculata.)*	[16] [19]

3.5.1. Methyl Esterification

Methanol converts the saponifiable fraction of the throughput dry lipids to fatty acid methyl esters (FAME). Higher heating value (HHV) of the output is calculated based on a typical fatty acid profile of the chosen algae species as presented in Ramirez-Verduco et al. [47] and validated against reported values for the chosen algal species [47]. Heat, electricity, and materials use is calculated using parameters from Ecoinvent for methyl esterification of soybean oil [28].

3.5.2. Supercritical Methanolysis

Wet algal biomass at a concentration as low as 15% w/w [49] may undergo single-step lipid extraction and transesterification by methanol under supercritical conditions (255 °C and 1200 psi for 25 min according to the 2014 NAABB report [17]). The optimum wet algae to methanol ratio (weight/volume) is reported as 1:9 [17][50]; however, most of this is assumed to be recovered and/or re-used and the actual depletion of methanol is assumed to be the same as Ecoinvent v3.2's value for transesterification of soybean oil.

While Brentner et al. [13] reports a 98% lipid efficiency and comparatively low energetic requirements, the NAABB report [17] mentions an 84% lipid efficiency and higher energetic requirements, and the latter study was used as it is more recent and its objectives specifically include the characterization of process performance. The heat/electricity ratio from Brentner et al. [13] was applied to the NAABB report's parameter for total energetic requirement per mass of slurry throughput.

3.5.3. Pyrolytic Conversion

Whole algal biomass is pyrolyzed in the presence of zeolite and sodium carbonate to produce bio-oil, syngas, biochar, and an aqueous phase [8][17]. Feed biomass can be in a slurry at a concentration of at least 80% w/w [8]. The NAABB report [17] details their findings on optimized operating conditions for pyrolysis of *N. oculata* specifically as well as on characterization of the products; thus, yield fractions and product HHVs were drawn from this report. Parameters for heat, electricity, sodium carbonate and zeolite requirements were obtained from Bennion et al. [8]. The user may choose to burn the produced syngas and bio-char to displace some of the heat requirement. The aqueous phase product may also be recycled to displace some of the carbon and nitrogen requirements of algae cultivation as described by Bennion et al. [8], and there is assumed to be no detriment to algal productivity or fuel quality from doing so.

3.5.4. Hydrothermal Liquefaction (HTL)

HTL can convert wet algal biomass at concentrations as low as 5% w/w into bio-oil and hence does not require intermediate drying, dewatering, or extraction processes [51][16]. Jazrawi et al. [52] reports that the yield becomes essentially independent of biomass loading concentration above 5% w/w, which generally agrees with the findings of Valdez et al. [16]. The reaction takes place in and with water [16]. Based on the composition of influent biomass, HHV is calculated using the Dulong formula, and yield is calculated using one of three statistical regression models made available here for HTL of *N. oculata* by Leow et al. [19]. Although bio-oil percent mass as sulfur is required by the formula, sulfur is not tracked by the model; however, as the influence of sulfur percent is minimal in the formula compared to the other elements, it was assumed that the sulfur percent of bio-oil is the same as that of *N. oculata* biomass, and the value for this was drawn from Quinn et al. [14].

Energy use and sodium carbonate depletion are calculated using parameters reported in Bennion et al. [8] for an industrial-scale HTL operating at 310 °C and 10,500 kPa, although the user may instead choose to use enthalpies from steam tables for the relevant temperature and pressure (which gives similar estimates), as described in Valdez et al. [16]. The aqueous phase product is recycled for organic carbon and ammonium to supplement the carbon and nitrogen needs of the algae cultivation model, as described in Bennion et al. [8], and there is assumed to be no detriment to algal productivity or fuel quality from doing so. It is also possible to treat the aqueous phase product of HTL via catalytic hydrothermal gasification (CHG) to recover energy [53][17] (anaerobic digestion of this residue being infeasible due to its high nitrogen content [54]). The CHG option is also made available by using model parameters from GREET [20]. It is worth noting that an HTL-CHG installation of capacity 1 m^3/d algae slurry (20% w/w) or 200 kg/d dry algae in Reliance Industries, Ltd.'s Jamnagar, India plant was discussed by the NAABB report [17].

3.6. Stabilization and Hydroprocessing

Bio-oil produced by thermochemical conversion processes – namely pyrolytic conversion and hydrothermal liquefaction – needs further processing before use as fuel in an automobile engine.

Stabilization is done to prevent the bio-oil viscosity from increasing over time and involves treating with near-critical propane. Hydroprocessing consumes electricity and uses hydrogen gas in the presence of zeolite to remove nitrogen and phosphorus from stabilized bio-oil.

The material and energy requirements per unit mass of throughput bio-oil for both stabilization and hydroprocessing were adapted from Bennion et al. [8]. As the exact structural changes induced by these processes were not known, it was assumed that neither process significantly alters bio-oil HHV. While Bennion et al. [8] describes minimal mass losses for stabilization, with all of the resultant bio-oil and raffine being sent to hydroprocessing, the recovery rate for hydroprocessing is taken as the average of the four cases described in Elliott et al. [51]. The default parameter values for bio-oil stabilization and hydroprocessing are shown in Table A-4.

3.7. Fuel Distribution and Combustion

Transportation and distribution of biofuel are modeled according to the parameters provided by Bennion et al. [8] per unit mass of biofuel.

GREET [20] provides the user with estimates for emissions from the combustion of the selected fuel in the selected automobile engine, on the basis of either mass or energy content of fuel or work done by the automobile. Our combustion model uses the estimates provided by GREET [20] for the emissions from combustion of 'Renewable Diesel II – Algae Lumped Model' in an 'HD Truck: Combination Short-Haul CIDI - RDII 100 from Distributed Standalone Bio-refinery' on a per MJ basis, and converts these to a per kg basis using HHV of Renewable Diesel – II reported by GREET [20].

Using these estimates, our model scales emissions to scenario-specific mass of biofuel combusted per functional unit of the analysis. It is assumed that the combustion properties of algal biodiesel resemble those of GREET's Renewable Diesel – II (algae lumped model). NO_x emissions are likely to scale well with mass, since most of the NO_x is formed by oxidation of

atmospheric nitrogen, but CO_2, CO, and CH_4 emissions are scaled to the estimated carbon content of fuel.

The default parameters used for fuel distribution and combustion process models are shown in Table A-5.

3.8. Anaerobic Digestion and Wastewater Treatment

Residual biomass is sent to an anaerobic digester, in which microbes break down the biomass in the absence of oxygen to produce digestate and biogas. The produced biogas is combusted in a combined heat-and-power system to recovery energy. Emissions of CO_2, CO, and CH_4 are considered from the biogas combustion. Carbon flow and process requirements and output of both heat and electricity are modeled using parameters from GREET. While anaerobic digestion (AD) is possible for non-lipid residue from esterification, the residue from HTL has a nitrogen content too high for AD [54].

Wastewater treatment was modeled using resource use and impacts for ‘wastewater from vegetable oil refinery’ as in Ecoinvent v3.2 [28]; carbon-based flows were scaled to the carbon content of input wastewater.

CHAPTER 4. INTEGRATED SYSTEMS MODEL CONFIGURATION

This section describes the functional unit and system boundaries, the cultivation model, the illustrative scenarios, and the allocation of co-products.

4.1. Functional Unit and System Boundary

The functional unit of this analysis is 1 MJ of diesel fuel. The system boundaries include everything from biomass cultivation through fuel conversion and combustion including the treatment of co-productions. This "well-to-wheel" boundary was selected to facilitate comparisons with other conventional fuels and biofuels including differences in fuel composition and energy content.

4.2. Default Algae Cultivation Model

While the framework is generalizable and can be applied to various algal species and cultivation systems, the illustrative scenarios use *Nannochloropsis oculata*. Sukarni et al. [6] reported *N. oculata* to be a viable biofuel feedstock due to its thin and relatively easily permeable or dissoluble cell wall, its high volatile matter content (67.4 wt.%), low moisture content (4.0 wt.%), and high energy content (16.80 MJ/kg).

The model used to simulate outdoor PBR growth of *N. oculata* in CO_2-enriched seawater media as described in Section 3.3 uses a harvest concentration set to 3 g/L as in Quinn et al. [14]. A range of 1 to 6 g/L has been reported for industrial-scale outdoor PBR growth of *N. oculata* [55]. An initial inoculum is assumed grown up to 1 g/L as described in Quinn et al. [14] and serial batches of this (drawn from harvests) may be used without detriment to productivity, reportedly for over a year [55].

4.3. Scenarios Constructed

Several factors were considered in constructing the illustrative production chains analyzed in this study. A baseline scenario was composed of existing, conventional technologies. Alternative scenarios with production chains that are potentially implementable soon were identified by considering the technologies' reported promise with respect to energy return and impacts. All scenarios were modeled for four coastal US cities, chosen for mutual geographical distance to represent distinct US weather conditions: 1) Blaine, WA; 2) Linden, NJ; 3) Richmond, CA; and 4) Galveston, TX. NSRDB weather data (i.e., air temperature, air pressure, relative humidity, wind velocity, and GHI in half-hour time steps) from 2015 was used. Each scenario's production chain is described in Table 6 and is followed by fuel distribution and combustion (process models described in Section 3.7).

Table 6. Biofuel production pathways for the six illustrative scenarios.

Scenario	Algae Cultivation	Harvesting	Dewatering	Drying	Lipid Extraction	Fuel Conversion	Residue Treatment
A. Baseline	Flat-Plate PBR	Disc-Stack Centrifuge		Spray Dryer	Hexane Extraction	Methyl Esterification	Anaerobic Digestion
B. RWWTF[1]		Electroflocculation + Dissolved Air Flotation	Disc-Stack Centrifuge	Spray Dryer	Hexane Extraction	Methyl Esterification	
C. SCM		Electrocoagulation	Belt Press Filter	Supercritical Methanolysis			
D. WHE		Electroflocculation + Dissolved Air Flotation	Chamber Pressure Filter	Wet Hexane Extraction		Methyl Esterification	
E. Pyrolysis		Electrocoagulation	Belt Press Filter	High-Intensity Dryer (Delft TU)	Pyrolytic Conversion + Stabilization + Hydroprocessing		Nutrient Recovery
F. HTL		Electrocoagulation	Chamber Pressure Filter	Hydrothermal Liquefaction + Stabilization + Hydroprocessing			

[1]Repurposed Wastewater Treatment Facility

A. Baseline Scenario The baseline scenario is meant to represent a system comprised of conventional industrial-scale processes that could be readily used in a microalgae-to-fuel system. Life-cycle studies of algae biofuels typically use pathways based on methyl esterification of extracted lipids as their baseline [18][56][10][13], since this is a mature technology that has been described as the "gold standard" for vegetable oil conversion [57]. Many studies have found that dewatering and drying are typically the largest contributors to global warming potential and cumulative energy demand [8][15][12][3], so it was decided to construct a baseline that requires these processes. As illustrated in Table 6, the production chains for the SCM, WHE, and HTL scenarios do not require a dedicated drying step. A baseline scenario that uses an energy-efficient drying technology facilitates comparisons with scenarios that reduce or eliminate the need for drying. Scenario A will therefore send PBR-cultivated algae to centrifugation and spray drying followed by dry hexane extraction of lipids, which are then converted to fatty acid methyl esters (FAME) using methanol. The non-lipid residue is sent to an anaerobic digester.

B. RWWTF Scenario: Milledge et al. [15] reports that chemical coagulation followed by dissolved air flotation is the most commonly used method of algae removal in wastewater treatment facilities. Shi et al. [41] noted the wide use of electroflocculation in wastewater treatment, and conducted experiments on a combined electroflocculation and dissolved air flotation process. A process chain is therefore included to assess the potential performance of such facilities as repurposed for algal biofuels manufacture, using electroflocculation (rather than chemical coagulation, in consideration of environmental performance [18]) as well as dissolved air flotation (electroflocculation and dissolved air flotation are modeled as a combined harvesting process based on data from Lee et al. [36]). The harvested algal slurry is further dewatered and dried using centrifugation and a spray dryer to achieve the concentration necessary for dry hexane extraction (assumed 90% w/w based on minimum output concentration of typical algae slurry dryers [39][42][43]). The other processes (i.e., cultivation, lipids extraction, fuel conversion, and residual treatment) are the same as in Scenario A.

C. SCM Scenario: In this scenario, supercritical methanolysis (SCM) eliminates the need for biomass drying and lipid extraction, and instead converts wet algae to biofuels using an excess of methanol at supercritical conditions (e.g., 255 ºC and 1200 psi for 25 min. [17]). Brentner et al. [13] evaluated a scenario that used only chitosan flocculation to concentrate the slurry prior to

fuel conversion via SCM. However, Pahl et al. [39] reported that chitosan flocculation could concentrate algal slurry to a 'maximum feasible' concentration of 25 kg/m^3 (~2.45% w/w), and the maximum concentration achieved by any of the chemical flocculation processes described by Fasaei et al. [39] is 8% w/w. The minimum concentration of algae reported in the literature that could be converted using the modeled process parameters for SCM is 15% w/w [49]. Therefore, our SCM scenario used electrocoagulation and belt press filtration to bring slurry concentration to 18 % w/w. Non-lipid residue is sent to an anaerobic digester.

D. WHE Scenario: Valicor's 'AlgaFrac' process for wet hexane extraction (WHE) of lipids is discussed in multiple life-cycle studies [9] [10]. It eliminates the need for an upstream drying step with its integrated flocculation and belt press drying, but the chemical composition of the flocculating agent is not reported. Although the process is reported by Gehrer et al. [9] to involve "complex additional procedures consisting of pretreatment, extraction, solvent recovery, oil separation, belt filter press and feed dryer," NAABB reports that the process is both reliable and scalable [17]. To model a production pathway that used WHE, the cultivated algae culture is harvested and concentrated using electroflocculation, dissolved air flotation, and a Netzsch chamber pressure filter to achieve a concentration between 22 and 27 % w/w. The extracted lipids are then converted to methyl esters, and the non-lipid residue is sent to an anaerobic digester.

E. Pyrolysis Scenario: Both Bennion et al. [8] and Richardson et al. [18] describe a scenario using single-step dewatering supplemented by a drying step before sending the whole algal biomass to pyrolytic conversion. Richardson et al. [18] found it to be the best production chain among the alternatives they studied. However, Bennion et al. [8] conclude that it is an energetically infeasible scenario that is outperformed by hydrothermal liquefaction. Scenario E sends the PBR-cultivated *N. oculata* culture to electrocoagulation, with subsequent application of a Bellmer belt press filter and the Delft TU high-intensity dryer (Table 4) to meet the 80% w/w concentration requirement of the pyrolytic conversion reactor. To offset some of the heating requirement, the biochar and syngas produced by pyrolysis are combusted and the generated heat is recovered using separate heat exchangers. The aqueous phase product is used for nutrient recovery (for algae cultivation) and only bio-oil is recovered for stabilization and hydroprocessing.

F. HTL Scenario: While the hydrothermal liquefaction (HTL) process can convert whole algal biomass into fuels, the yield and quality of these fuels depend on the process conditions as well as on the composition and dry weight concentration of the influent algal slurry [19][52]. Previous studies exploring HTL have reported a high energy return on energy investment (EROEI) for the HTL process itself (e.g., 5 to 11 [16]), but cite the need to incorporate upstream processes to estimate the net EROEI and overall environmental performance of production chains that include HTL [16][58][19]. Bennion et al. [8] performed a well-to-pump LCA that estimated negative overall GHG emissions and an EROEI of about 0.81. In this scenario, the PBR-cultivated *N. oculata* culture is harvested via electrocoagulation, followed by supplemental dewatering using a Netzsch chamber pressure filter before HTL of slurry. Bio-oil is recovered for stabilization and hydroprocessing, while gaseous products are combusted on-site for energy recovery. Nutrients are recovered from the aqueous phase product and re-utilized in algae cultivation.

4.4. Handling of Co-Products

The on-site energy recovery from any products of anaerobic digestion will offset cumulative energy demand as calculated from the Ecoinvent v3.5 life-cycle inventory database [28]. If the user chooses to immediately burn the biochar and syngas formed during pyrolysis, the equivalent amount of heat is recovered to process flows and carbon dioxide is released to the atmosphere. About 98 to 99% of seawater input to harvesting and dewatering processes is recovered for use as media.

Glycerine is produced during methyl esterification of lipids (conventionally or by supercritical methanolysis), and there are no on-site processes that require it. Glycerine can be burned to produce energy, and the emissions and energy produced from burning various grades of glycerine were modeled based on the parameters reported by Bohon et al. [59]. In some situations, glycerine could be sold as a co-located by-product.

A 2008 study conducted by Argonne National Laboratory [60] discusses the handling of co-product credits for a selection of renewable fuel production processes. Their hybrid approach suggests an offset credit for avoided production of residual cake as well as glycerine. The study also considered allocating impacts between co-products based on either their market values or

their energy contents. To facilitate comparisons with GREET's impacts from conventional fuels, the LCIA results presented in this study give an offset credit for avoided glycerine production, with the emissions and resource use associated with US production of glycerine by esterifying soybean oil developed from Ecoinvent v3.5 [28]. The effects of choosing alternative approaches for handling glycerine impacts (namely combustion for heat recovery and co-product allocation based on market value) are illustrated in Figure A-1 in the appendix.

CHAPTER 5. RESULTS AND DISCUSSION

5.1. Cultivation Model Results

The settings discussed in Section 4.2 were used in the PBR algae cultivation model described in Section 3.2. It was found that among the four analyzed locations (Section 4.3), Richmond, CA had the highest productivity for 2015 weather data, and therefore is used as the standard location for the presentation of results. Air temperature, PBR temperature, and biomass concentration results for each of the four seasons in the 2015 NSRDB weather data for Richmond, CA are shown in Figure 3.

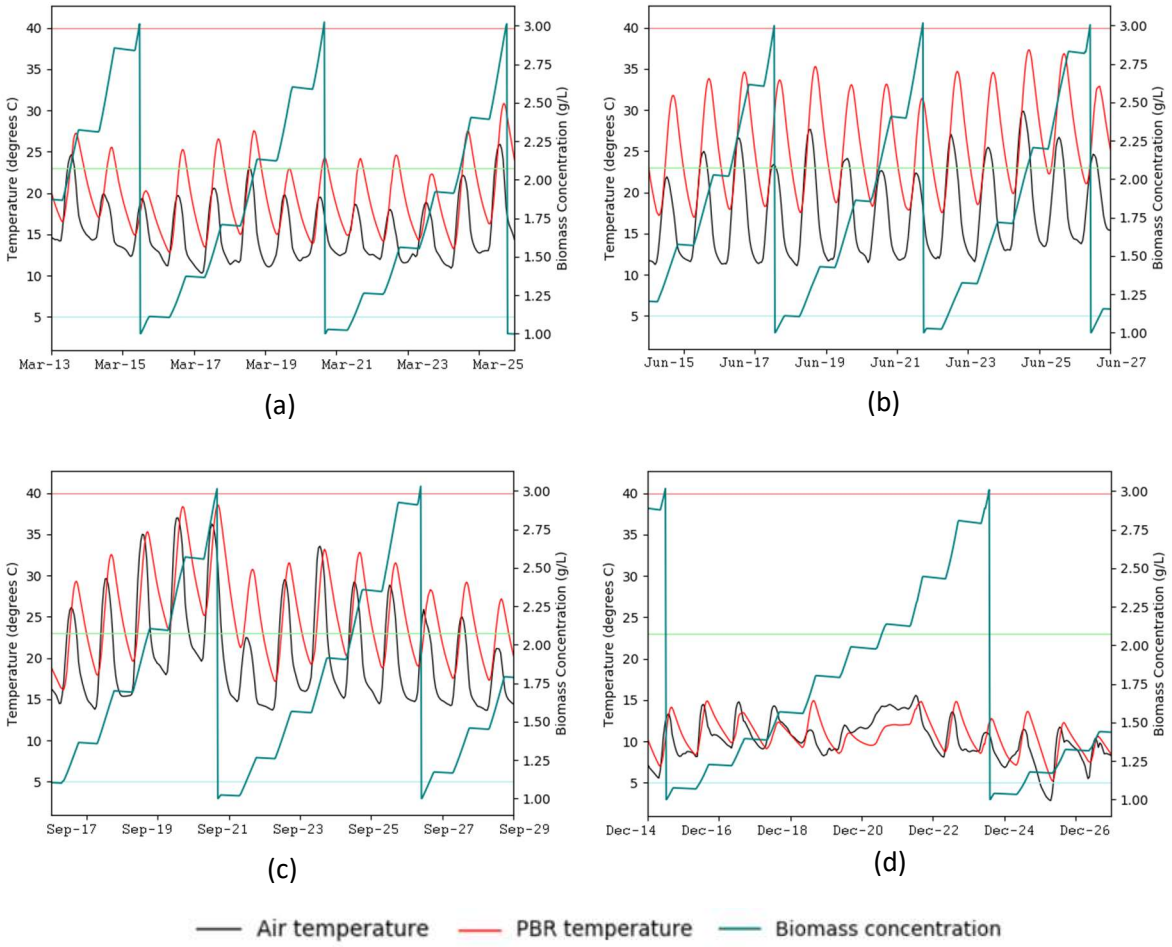

Figure 3. Model results for the cultivation of *N. oculata* using 2015 weather data from NSRDB for Richmond, CA, without supplemental heating or cooling. Plotted are air temperature data from NSRDB and model estimates for PBR temperature and biomass concentration for timespans in 2015 that include the (a) March equinox, (b) June solstice, (c) September equinox, and (d) December solstice. The lighter blue, green, and red lines parallel to the x-axis represent respectively the minimum, optimum, and maximum temperatures for algae growth.

The dependence of growth rate on weather is evident from Figure 3; the algae grow fastest during the summer solstice period (~4 days per harvest) (Figure 3 (b)); harvest frequency decreases during the spring and autumnal equinoxes (~ 4.5 and 5 days per harvest) (Figure 3(a) and Figure 3(c)) and drops sharply during the winter equinox (~9 days per harvest) (Figure 3(d)).

The effect of introducing supplemental electrical heating and cooling was also evaluated. However, the addition of supplemental heating and cooling increases the electricity demand from cultivation by 110%, and only increases the biomass production by 3.2% (Table 7). Since the

heating and cooling was only used ~3 days per year, the use of a regionally feasible, less energy-intensive source of temperature control (e.g., air humidifiers during hot, dry weather) may be worth considering.

Table 7. Annual life-cycle inventory results for the cultivation of *N. oculata* in 16 PBRs each of dimensions 17.4 m x 0.08 m x 0.3 m using 2015 weather data from NSRDB for Richmond, CA as part of the HTL scenario.

Inventory	**Without temperature control**	**With temperature control**	**Unit**
Output biomass	740	764	kg
lipids	303	312	kg
carbohydrates	296	306	kg
protein	141	146	kg
total carbon content	370	382	kg
total nitrogen content	30	31	kg
Output seawater	247	255	m^3
total solids	0.294	0.294	% w/w
Seawater input from recovery	244	252	L
Additional seawater treated before use	2.96	3.06	m^3
Electricity used	86.5	181.4	kWh
for mixing	74.7	74.9	kWh
for pumping harvests	11.8	12.2	kWh
for supplemental heating	0.0	20.7	kWh
for supplemental cooling	0.0	73.6	kWh
Diammonium phosphate used	2.0	2.1	kg
Urea used	23.2	23.9	kg
N recovered from downstream	18.3	18.9	kg
CO_2 used	1180	1215	kg
C recovered from downstream	49.0	50.5	kg
PBR footprint (land use factor of 2)	108	108	m^2
Operational time	364.125	365.0	days
Number of harvests (at 3 g/L)	63	65	#

5.2. LCIA Results

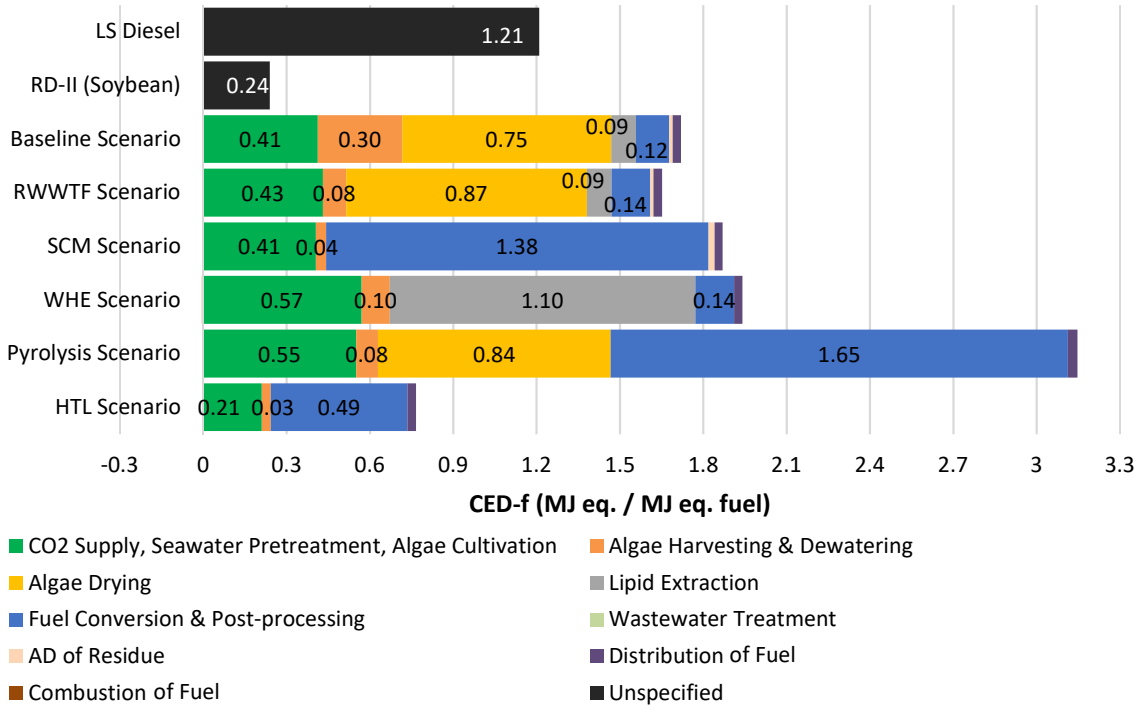

Figure 4. Process contributions to cumulative energy demand from fossil fuels for each transportation fuel. Impact data for low-sulfur diesel (LS Diesel) and Renewable Diesel – II (RD-II) were adapted from GREET (2018) and are not illustrated on a process level. Direct electricity use was modeled as sourced from a 100% fossil electricity grid.

Using the impact factors described in Section 2.2, impacts were estimated for the six scenarios described in Section 4.3. Since each scenario describes a facility that imposes added demand on the U.S. electrical grid, the source of electricity used was a 100% fossil marginal electricity mix (see Figures 4, 5, and 7), in which the added demand to the grid is met by added supply from coal and natural gas. The effect of changing the electrical source to the average U.S. mix or to a renewable electricity source mix are evaluated and discussed further in the section.

As shown in Figures 4 and 5, when using the marginal electrical grid mix, only the HTL scenario outperforms conventional diesel in terms of CED-f or GWP. The use of soybean-based biodiesel leads to 55% reduction in GHG emissions compared to the HTL scenario. As discussed in Section 4.3, the Baseline and RWWTF scenarios suffer due to high heat requirement for slurry drying.

The constructed WHE and SCM scenarios attempt to replace energy-intensive dewatering and drying steps with single-step processes for either lipid extraction or fuel conversion. However, the replacement processes also require significant amounts of heat, electricity, and materials (e.g. hexane, methanol), and hence do not improve either scenario's CED-f or GWP impacts compared to the Baseline scenario.

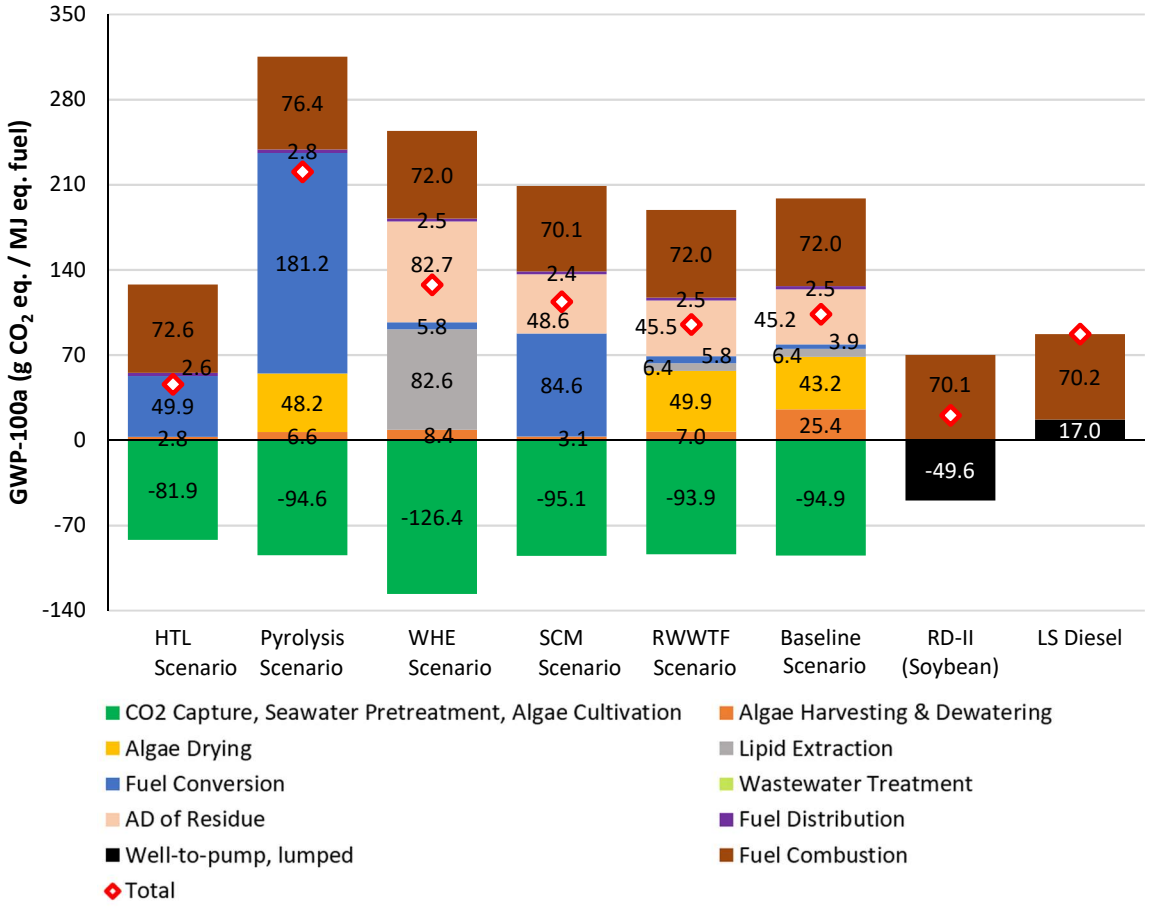

Figure 5. IPCC Global Warming Potential impact over a 100-annum period for each transportation fuel for well-to-wheel system boundaries. Impact data for low-sulfur diesel (LS Diesel) and Renewable Diesel – II (RD-II) were adapted from GREET (2018). Direct electricity use was modeled as sourced from a 100% fossil electricity grid.

The Pyrolysis scenario slightly reduces the drying requirement compared to the Baseline and RWWTF scenarios, since it converts 80% w/w whole algal biomass slurry to bio-oil. However, the reported bio-oil yield is only ~29% d.w. [8], compared to ~ 36% d.w. FAME yield on dried biomass (~89% d.w. FAME yield on lipids [28]) for methyl esterification. The Pyrolysis

scenario's production chain also adds significant heat, electricity, and material requirements over the baseline and RWWTF scenarios for pyrolytic conversion, stabilization, and hydro-processing. These requirements overwhelm the benefits from energy recovery from on-site combustion of syngas and biochar. The Pyrolysis scenario has the greatest fossil energy requirements as well as GHG emissions of the scenarios considered. Due to a low HHV (36 MJ/kg [17]), it also has the greatest combustion emissions despite a relatively low carbon content (73% w/w [17]).

The HTL scenario performs the best among the microalgae biofuel scenarios by converting whole algal biomass without the need for slurry drying past 15% w/w (24.5% w/w output of Netzsch chamber pressure filter was used for the HTL scenario). The fuel yield calculated based on biomass composition is 54.5% d.w., which is within reported yields of 33 – 68% d.w. for *N. oculata* [19]. The energy required by the conversion process is significantly offset by energy recovery from burning process gases as described in Bennion et al. [8]. Stabilization and hydroprocessing are significant contributors to CED-f, respectively about 16% and 23%. The absolute contribution of cultivation in the HTL scenario is significantly lower than for other scenarios because of the high bio-oil yield of HTL, since the absolute impacts are divided by a relatively large quantity of fuel produced. The calculated fuel HHV of 38.9 MJ/kg is slightly lower than for biodiesel produced by methyl esterification (39.8 MJ/kg [48]) or supercritical methanolysis (42 MJ/kg [17]), and significantly lower than for low-sulfur diesel (45.6 MJ/kg) and soybean-based renewable diesel-II (46.8 MJ/kg); however, the HHV is only slightly lower than the HHV range of 39 – 42 MJ/kg reported for biodiesels from vegetable oil [61].

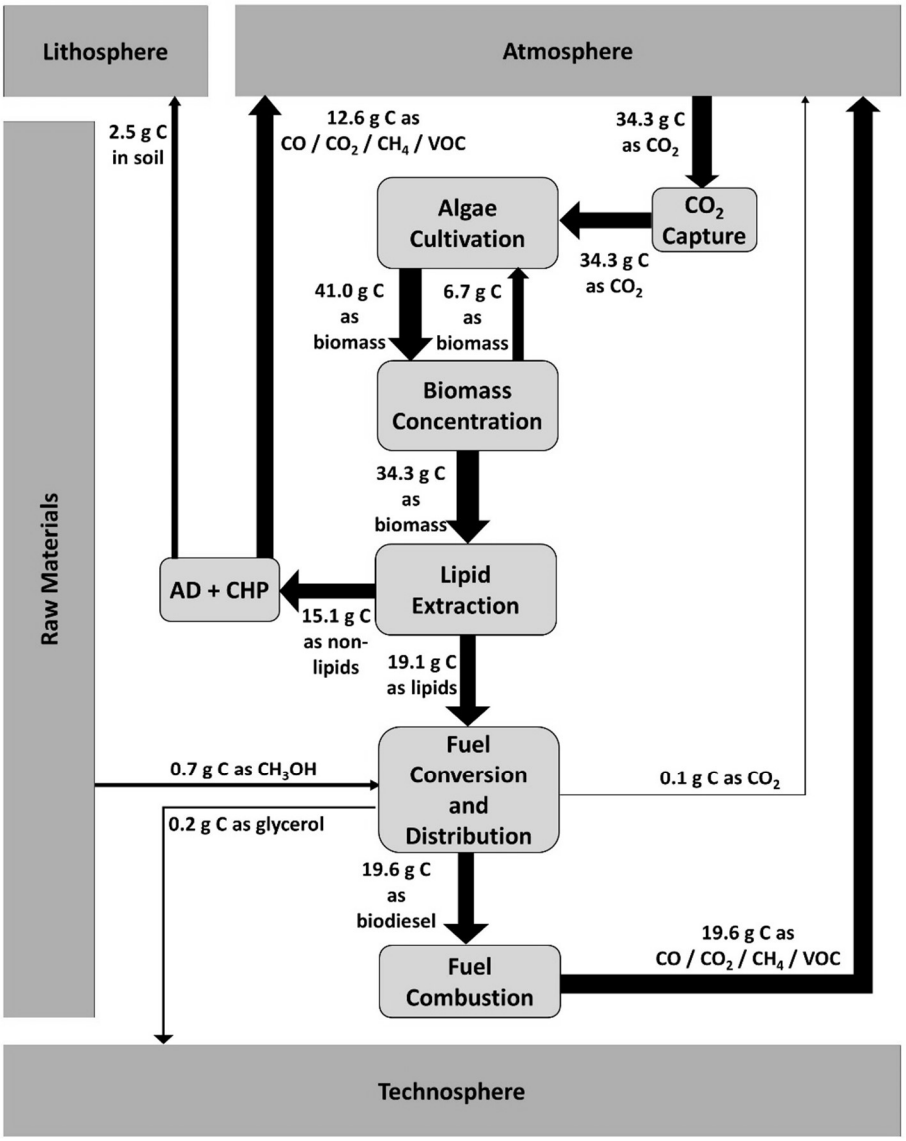

Figure 6. Flow of carbon through the production-and-use chain in the RWWTF scenario.

The flows of carbon in and out of the systems for the RWWTF scenario are illustrated in Figure 6. Most of the carbon (98%) enters the systems as CO_2 used during cultivation and is returned to the atmosphere mainly via combustion (56%) and anaerobic digestion (36%). Approximately 7% of the input carbon is sequestered in soil after residual biomass is sent for anaerobic digestion.

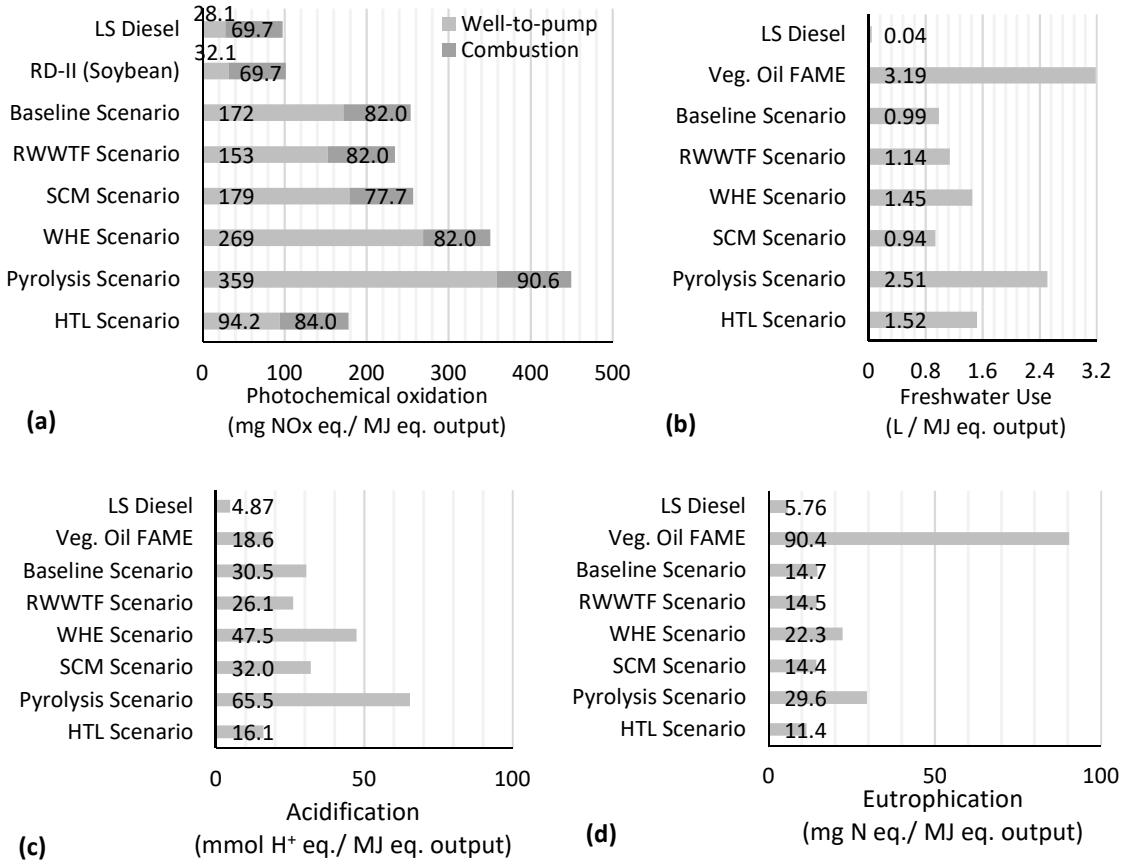

Figure 7. (a) Photochemical oxidation, (b) freshwater use, (c) acidification, and (d) eutrophication impacts for each transportation fuel for well-to-wheel system boundaries. Photochemical oxidation impacts for Low-Sulfur Diesel (LS Diesel) and Renewable Diesel – II: Soybean were developed from GREET (2018). Impacts in (b) – (d) for market for LS Diesel and vegetable oil FAME (veg. oil FAME) were developed from Ecoinvent v3.5. Direct electricity use was modeled as sourced from a 100% fossil electricity grid.

In Figure 7 (b) – (d), low-sulfur diesel and vegetable oil FAME impacts were adapted from Ecoinvent v3.5, since GREET does not consider these impacts. While low-sulfur diesel performs best in each of the impacts displayed due to relatively low electricity and fuel required to produce it, vegetable oil FAME has greater freshwater use and eutrophication impacts than any of the algal biofuel cases analyzed, higher by a factor of ~2 and ~8 higher respectively than those of the HTL scenario. This is due mainly to the high water and fertilizer use for growth of terrestrial crop feedstock. Acidification associated with the HTL scenario is also ~14 % lower than that associated with vegetable oil FAME.

Fossil electricity is the largest contributor to the photochemical oxidation impact of the baseline, RWWTF, SCM, and WHE scenarios, followed by urea production for use in PBRs. However, the two scenarios using thermochemical pathways for biomass conversion to bio-oil (HTL and Pyrolysis) require hydroprocessing, and production of the required hydrogen dominates the photochemical oxidation impacts of these scenarios.

Urea production for use in PBRs is a significant contributor to freshwater use. In the pyrolysis and HTL scenarios, however, hydrogen production for bio-oil processing dominates freshwater use, and these two scenarios have the largest freshwater use impacts among the algal biofuel cases. Another significant contributor to freshwater use is the production of soda ash (Na_2CO_3) for use in the HTL process.

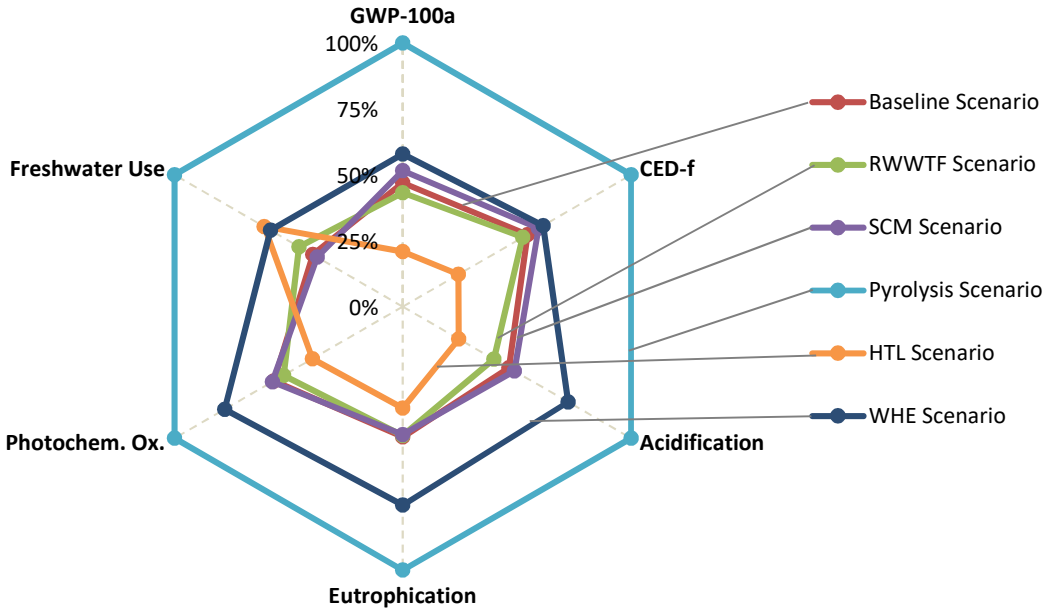

Figure 8. Normalized environmental impacts of all scenarios. 100% corresponds to the highest environmental impact among the six algal biofuels scenarios; the magnitude of each environmental impact is represented by its distance from the central point (0%).

Figure 8 is an illustrative comparison of the environmental impacts of the six algal biofuels scenarios analyzed. Environmental impacts – including those shown in Figures 4, 5, and 7 – are each normalized to 100% based on the maximum impact. Since the Pyrolysis scenario performed the worst in every impact category, each of its impacts are at 100%. The HTL scenario

performed the best in impacts other than freshwater use and the other scenarios generally performed similarly to one another.

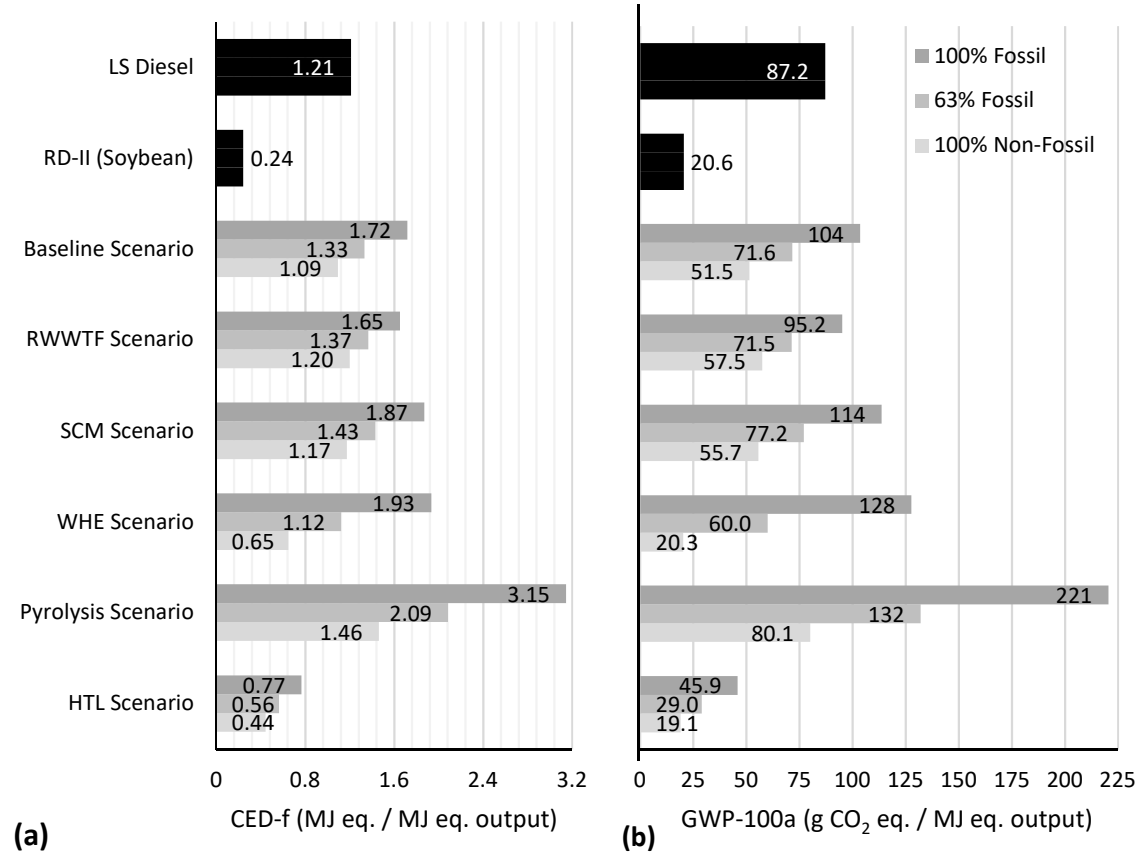

Figure 9. (a) Cumulative fossil energy demand and (b) global warming potential for each transportation fuel based on the direct electricity source used. 100% Fossil represents the US marginal grid mix, 63% fossil represents the US average grid mix, and 100% Non-fossil represents a potential low-carbon future mix from the grid or on-site production.

Reducing the fraction to the direct electricity mix from fossil sources reduces the fossil energy demand and GWP. On-site production of non-fossil electricity is worth considering, and could improve the sustainability of microalgae-to-biofuel systems using readily available technology [62].

However as seen in Figure 9, even with a 100% non-fossil grid source for the direct use of electricity, only the HTL and WHE scenarios are comparable to soybean-based biodiesel in terms of GWP, and both still use 1.8 – 2.7 times as much fossil energy. Impacts from the Pyrolysis scenario are greatly reduced but as the initial impacts are high and the most significant

contributor is heat use rather than electricity use, it still has the highest impacts among algal biofuels; however, the GWP of even the Pyrolysis scenario with a 100% non-fossil grid outperforms that of low-sulfur diesel.

The changes to photochemical oxidation and freshwater use by altering the direct electricity source mix are illustrated in Figure A-2 in the appendix.

5.3. Sensitivity Analysis Results

An 8000-iteration Monte Carlo simulation was performed for each scenario and Spearman correlation coefficients were calculated for each input and output.

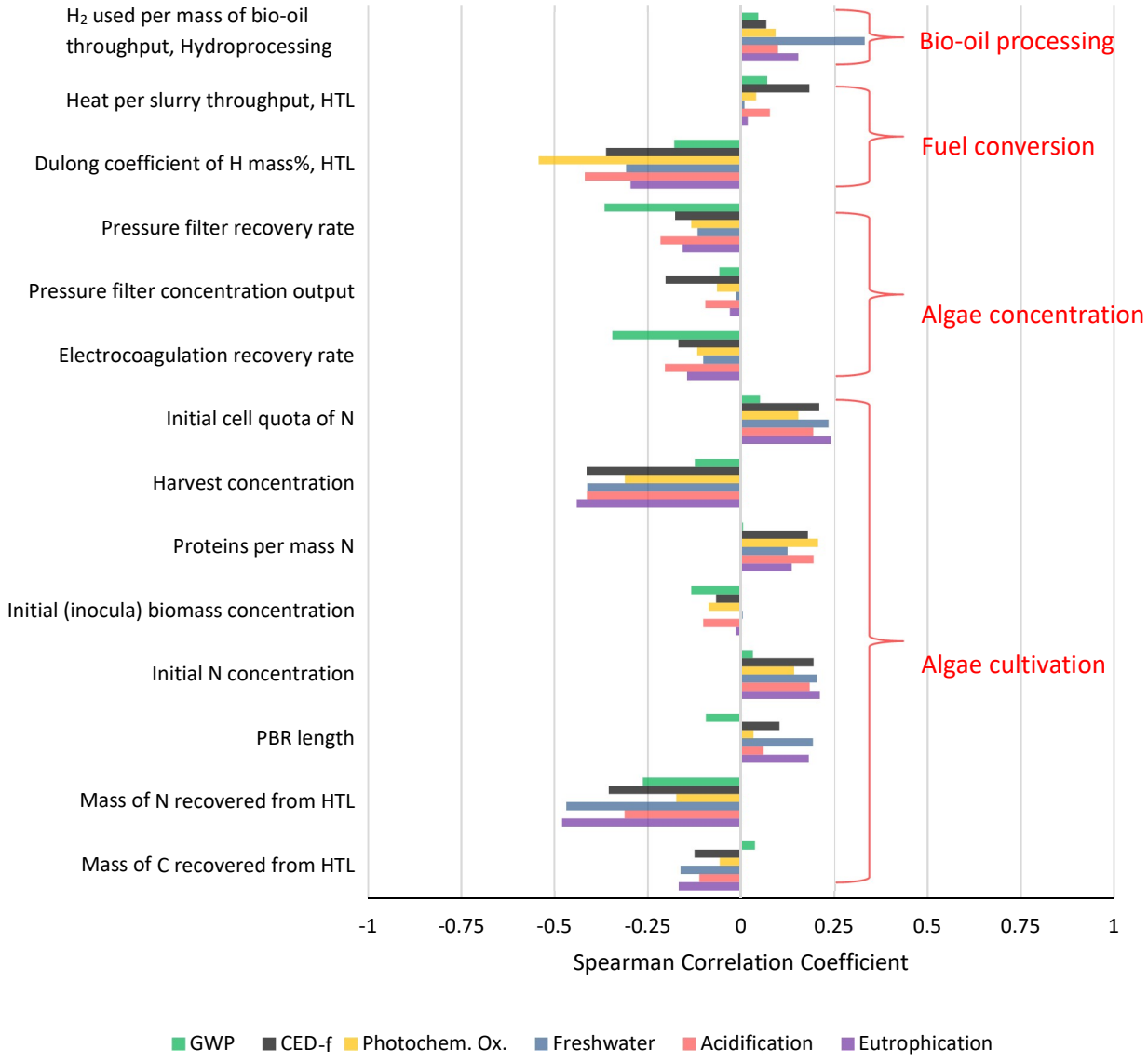

Figure 10. Spearman correlation coefficients of the most significant model parameters in the HTL scenario for individual environmental impacts. Direct electricity use was modeled as sourced from a 100% fossil electricity grid.

As illustrated in Figure 10, the most significant parameters for the HTL scenario were HTL process heat use, output concentration from and biomass recovery rates of algae concentration, nutrient recovery parameters, and productivity-related parameters (e.g. algae harvest

concentration, constant carbohydrate content, and initial N quota). The collective effect of varying the productivity-related inputs was the most significant among these parameters. Increasing the set harvest concentration during algae cultivation reduces the overall impact, since fewer harvests (from the same total PBR volume) are required to be pumped, concentrated, and converted via HTL; however, as the growth model was reportedly validated only for a 3 g/L harvest concentration [14], and the assumptions made to characterize the effect of light intensity are only valid for lower concentrations, this effect was not further explored by this study. It can be safely said, however, that increasing set harvest concentration from 1 g/L to 3 g/L increases PBR mixing energy use but significantly decreases the load on the slurry concentration processes downstream of cultivation, and the optimum set harvest concentration may depend on weather parameters and algae species. Decreasing the constant carbohydrate content and initial N quota reduces carbohydrate and protein content of biomass, thereby increasing the energy-rich lipid fraction. The dewatering output concentration and HTL heat parameters dictate heat required by the HTL process. Recovery rates of process steps with the most biomass throughput (harvesting, dewatering) significantly affect the functional quantity of biofuel.

Figure 11 (d) shows productivity results for the four locations analyzed. Richmond, CA had the highest biomass productivity, followed by Blaine, WA and Galveston, TX. The average GHI of these locations is reported as 4.89, 3.48, and 4.79 $kWh/m^2/d$ respectively [63]. Studies often use GHI exclusively to estimate areal algae productivity [64][65]. It is evident in the higher productivity of Blaine, WA over Galveston, TX, as well as the disproportionately higher productivity of Richmond, CA, that the sole use of average GHI does not always yield reliable estimates of productivity.

However, the environmental impacts were only marginally lower for Richmond, CA than for the other locations analyzed, because changes in productivity led to relatively small changes in environmental impacts at productivities above ~ 15 $g.m^{-2}.d^{-1}$ (Figure 11). Only land use (which is not assessed in this study, as not every technology's footprints could be estimated based on what is reported in the published literature) would be significantly higher for the other locations.

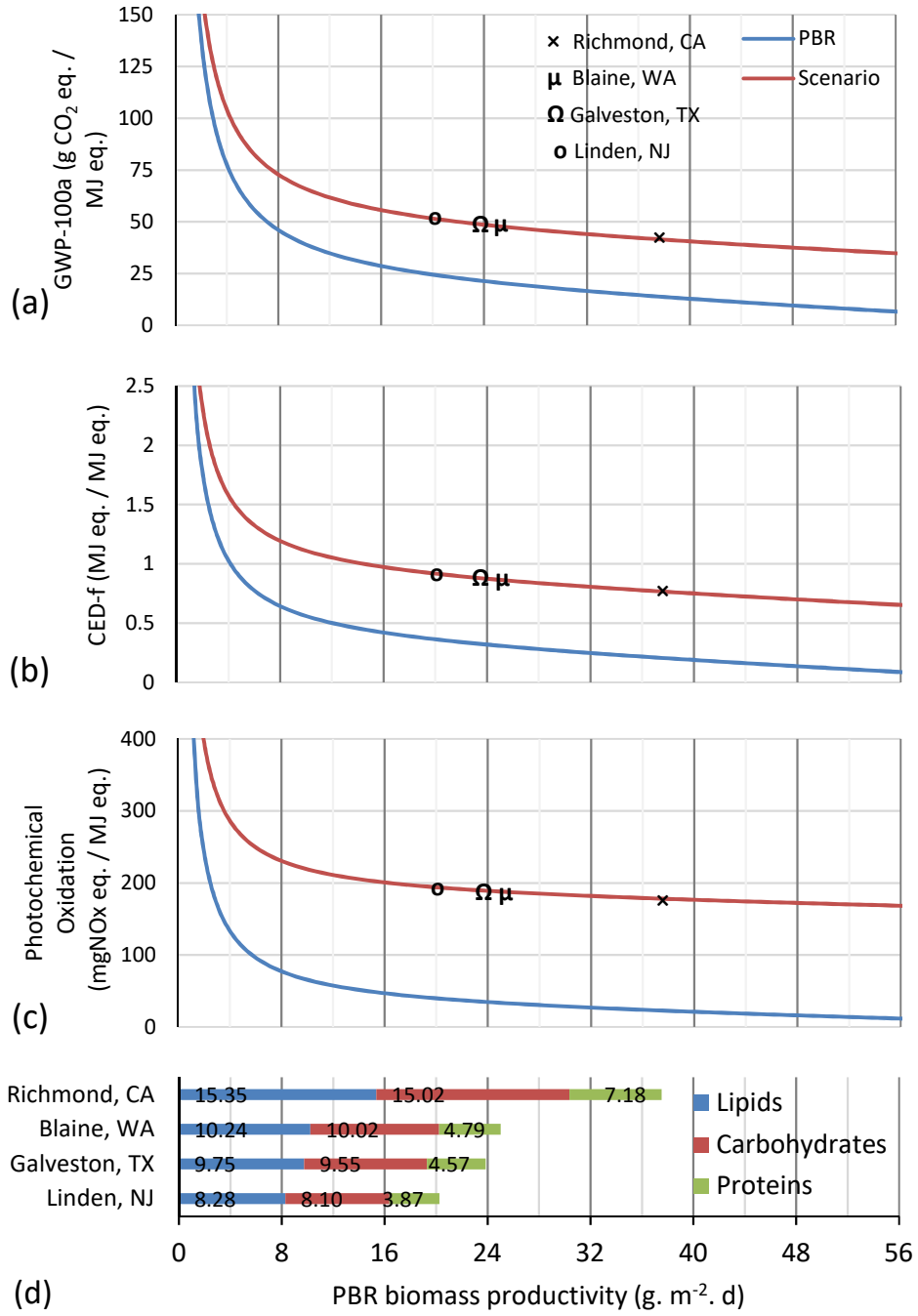

Figure 11. For the HTL Scenario (a) Global Warming Potential, (b) Cumulative Energy Demand – Fossil Fuels, and (c) Photochemical Oxidation impacts (well-to-wheel) are plotted against biomass productivity. The photobioreactor biomass productivity and composition for four locations is displayed in (d). Direct electricity use was modeled as sourced from a 100% fossil electricity grid.

To more directly characterize the influence of biomass productivity on impacts, the growth rate – and consequently the productivity – of *N. oculata* was varied in the PBR cultivation model. It was modeled for media to be harvested when the same biomass concentration of 3 g/L was achieved, meaning harvesting frequency is increased. Figure 11 illustrates the change in impacts (for the HTL Scenario) upon varying productivity in this manner.

As productivity increases from 3 to 15 $g.m^{-2}.d^{-1}$ a decrease of about 67 g CO_2 eq. (55%), 0.82 MJ eq. (45%), and 118 mg NO_x eq. (37%) is observed in global warming potential, cumulative energy demand from fossil fuels, and photochemical oxidation impacts respectively per functional unit of 1 MJ eq. However, a productivity increase from 15 to 30 $g.m^{-2}.d^{-1}$ nets a further reduction of only about 12 g CO_2 eq. (21%), 0.1 MJ eq. (10%), and 17 mg NO_x eq. (8%) respectively in those impacts.

Increasing PBR biomass productivity past 10 – 15 $g.m^{-2}.d^{-1}$ may not significantly improve environmental performance, except in terms of land use. This indicates that locations with lower productivities may still perform competitively with respect to environmental impacts and fossil energy demand. A much greater reduction in impacts is possible by sourcing direct electricity use from non-fossil sources or by improving the energy economy of the production chain. This agrees with the recommendation made by Collet et al. [62] to reduce impacts by using local renewable energy sources rather than improving productivity past what they deemed to be easily achievable values of 10 – 15 $g.m^{-2}.d^{-1}$.

It is worth mentioning here that Passell et al. [10] reported that, for the WHE-based production chain they analyzed, when the algae productivity estimate was changed from a "base case" value of 3 $g.m^{-2}.d^{-1}$ to a "future case" value of 25 $g.m^{-2}.d^{-1}$ (along with significantly increasing low-carbon electricity in the grid and reducing process requirements) GWP impact reduced by ~94% and CED-f reduced by ~96%.

Quinn et al. [14] noted that under nitrogen-starvation, *N. oculata*'s metabolism shifts from protein synthesis almost entirely to lipid synthesis. The PBR cultivation model developed by the study assumes a constant carbohydrate content of 40% d.w.; however, Quinn et al. [14] also reported that laboratory data suggests that carbohydrate content of *N. oculata* could fluctuate by as much as 10% ($\pm$4% d.w.) under nitrogen-starvation conditions. As discussed in Section 3.5.4,

the HTL model developed calculates bio-oil yield, carbon content, and HHV using input biomass composition. The effects of altering the carbohydrate content of *N. oculata* on the impacts of the HTL scenario were therefore analyzed.

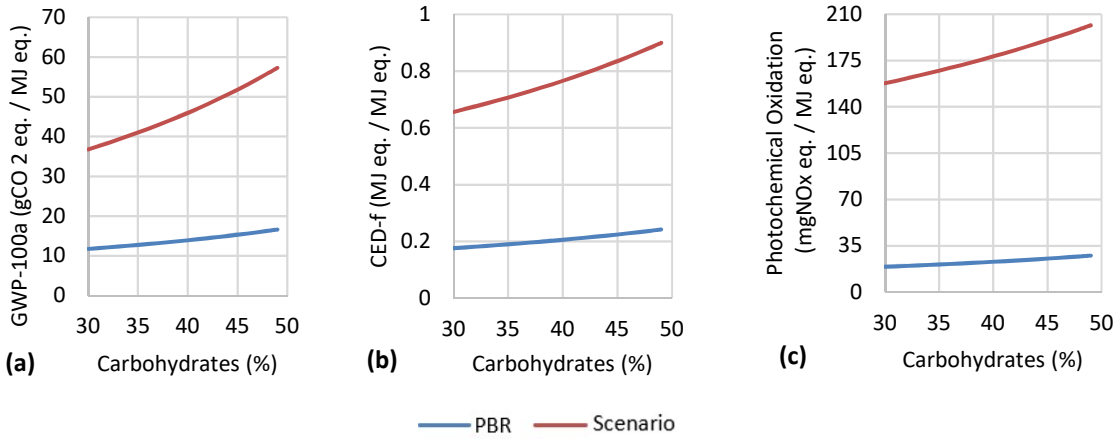

Figure 12. Effect on (a) GWP, (b) CED-f, and (c) Photochemical oxidation impacts of the HTL scenario on varying *N. oculata*'s constant carbohydrate content during PBR growth.

As illustrated in Figure 12, the HTL scenario impacts increase significantly with increase in carbohydrate concentration as bio-oil yield, carbon content, and HHV are all affected. The reported variation of ± 10% (± 4% d.w.) changes the scenario's impacts per 1 MJ eq. output as follows: GWP by + 4.6 to – 4.0 g CO_2 eq., CED-f by + 0.06 to – 0.05 MJ eq., and photochemical oxidation by + 9.7 to -8.7 mg NO_x eq.

HTL process heat use was not significantly higher than the steam table enthalpy differences [16][8], and so is already a fairly optimized parameter. It is therefore more feasible to attempt to improve parameters of upstream processes, such as dewatering output concentration. This reduces amount of water throughput to the HTL step and helps minimize HTL process heat use indirectly. We analyzed the effects of altering dewatering output concentration on HTL scenario impacts.

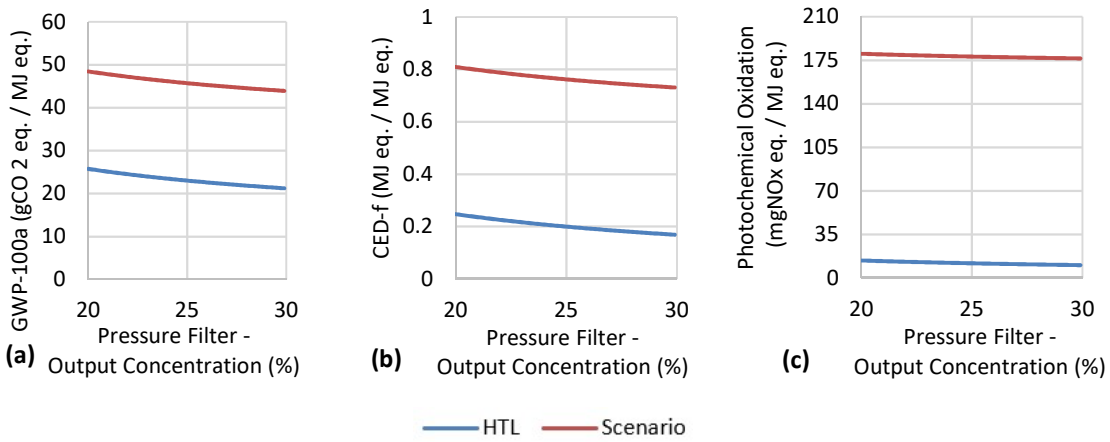

Figure 13. Effect on (a) GWP, (b) CED-f, and (c) Photochemical oxidation impacts of the HTL scenario on varying slurry concentration output by the Netzsch chamber pressure filter used in the dewatering step.

As was expected, impacts decreased as a decreasing amount of water was required to be heated in the HTL step; as HTL heat use was the largest single contributing inventory to GWP and CED-f and a significant contributor to most impacts, the decrease in impacts is almost linear within the plots observed in Figure 13. It is also worth noting that variation in parameters of earlier processes (e.g., the carbohydrate content of *N. oculata*) has greater effect on scenario impacts than varying parameters of latter processes such as the concentration of slurry input to HTL.

CHAPTER 6. CONSIDERATIONS FOR USE AND LIMITATIONS

LCAs conducted using this framework provide comparisons among alternative algal biofuels scenarios and against other fuels and biofuels. However, the results are not intended for making statements regarding the absolute environmental performance or sustainability of analyzed systems. Additionally, the default models currently implemented in the framework estimate the material and energy requirements only of facility operation, but not of facility construction and equipment installation. While new models can include these sub-processes, care should be taken to ensure that consistency is maintained across the process models. Also, while it was ensured that all process models used data for technologies intended for industrial throughput capacity, these capacities were not provided or made use of in the framework. For technologies with relatively small capacities, this may be especially significant since the construction, installation, and labor costs do not translate into the results reported here, and the assumptions made for the pumping energy use may not hold well.

The process models in the framework calculate the life-cycle inventory based on biomass composition as lipids, proteins, and carbohydrates as well as carbon and nitrogen content. However, the fatty acid distribution within the lipid fraction (which affects energy content) and the sulfur content (which is a criterion in fuel drop-in standards) are not tracked and process models instead use assumed values based on algal species where necessary. Additionally, data is not provided within the framework for growth parameters of algal species other than *N. oculata*, so additional models would need to be developed and implemented to assess other algae species. Many of the default parameters assessed in the Monte Carlo analysis do not have accurate statistical distributions, which would be necessary to more fully understand the probable life-cycle performance of the alternatives and which inputs most affect the variations in results. Lastly, while the source mix of electricity for direct use may be varied as demonstrated in Figures 9 and A-2, the framework is not set up to update the electricity-related emissions associated with the secondary materials and fuels used and produced by the processes. This would require updating the background life-cycle data used for these models.

CHAPTER 7. OBSERVATIONS, IMPLICATIONS, AND FUTURE WORK

A major contribution of this research is the development of an open-source life-cycle modeling framework capable of: (i) assessing and comparing the environmental performance of alternative microalgae-to-biofuel systems; and (ii) performing sensitivity analyses to assess the influence of individual model parameters on the environmental performance. The open-source, Python-based framework is modular and facilitates easy integration of existing as well as new technologies into systemwide analyses. This framework provides the functionality to characterize the influence of individual model parameters on the environmental performance of the fuel. It is the first open-source, modular framework for detailed spatiotemporal life-cycle modeling and analysis of algal biofuel production.

The framework is populated with a range of default process models for industrial-scale technologies. For example, the PBR cultivation model utilizes annual weather data from NSRDB to estimate changes in algal growth and composition in half-hourly intervals based on GHI and PBR temperature (which is estimated as a function of air temperature, air pressure, relative humidity, and wind velocity). Additionally, the HTL model calculates bio-oil yield, composition, and HHV as a function of input biomass composition.

The sensitivity analysis functionality offered by the framework enables users to identify significant parameters using Monte Carlo simulations and characterize their individual influences on the fuel's environmental performance. The results of this study's sensitivity analyses suggest that current technologies can provide energetically and environmentally viable pathways for microalgal fuel production the representative coastal US cities analyzed, especially with an increased fraction of low-carbon electricity for direct use by production facilities.

Additional research in cultivation technology may enhance the environmental performance of microalgal biofuels significantly by improving lipid yields of algae (e.g., by reducing the algae's carbohydrate content or initial nitrogen quota), or by increasing the concentration achievable by algae in a single harvest (which greatly reduces the load on process requirements that scale with slurry volume, such as algae dewatering, drying and thermochemical processes), even at the cost of areal biomass productivity to some extent. Results indicate that improving areal biomass productivity past values observed for the representative coastal US cities analyzed using models

of current cultivation technology may not significantly improve the environmental performance of microalgal biofuel.

There are several areas for potential improvements to the framework as well as future contributions using the framework. For example, new models can be implemented to further populate the tool, potentially including even more detailed models for algal growth kinetics validated for other harvest concentrations in several alternative reactor infrastructures (e.g. bubble column PBRs, open raceway ponds). This would enable future assessments to compare and recommend targeted potential improvements to harvest concentration and reactor structure and assess the effects of genetically regulating specific algae traits (e.g. to alter carbohydrate content, nitrogen quota, or lipid metabolism), and to better assess the influence of harvest concentration on environmental performance. Additionally, the cultivation model is already set up to read weather data for multiple locations, and this functionality could be used in future studies to estimate aggregated US biomass productivity and system environmental performance. These improvements to the framework would enable future studies to more quickly and meaningfully characterize the implications of their research at a system-wide level, and to make further recommendations for targeted improvements to processes involved in microalgal biofuel production. The framework may also be expanded to include other fuels, thereby prompting a deeper understanding of their environmental performance.

REFERENCES

[1] International Energy Agency, *World Energy Outlook 2019*

[2] U.S. Energy Information Administration 2016 *International Energy Outlook 2016* vol 0484(2016)

[3] Quinn J C and Davis R 2015 The potentials and challenges of algae based biofuels: A review of the techno-economic, life cycle, and resource assessment modeling *Bioresour. Technol.* **184** 444–52

[4] Davis R, Aden A and Pienkos P T 2011 Techno-economic analysis of autotrophic microalgae for fuel production *Appl. Energy* **88** 3524–31

[5] U.S. EIA 2019 Annual Energy Outlook 2019 with projections to 2050 *Annu. Energy Outlook 2019 with Proj. to 2050* **44** 1–64

[6] Sukarni, Sudjito, Hamidi N, Yanuhar U and Wardana I N G 2014 Potential and properties of marine microalgae Nannochloropsis oculata as biomass fuel feedstock *Int. J. Energy Environ. Eng.* **5** 279–90

[7] Quinn J C, Catton K, Wagner N and Bradley T H 2012 Current Large-Scale US Biofuel Potential from Microalgae Cultivated in Photobioreactors 49–60

[8] Bennion E P, Ginosar D M, Moses J, Agblevor F and Quinn J C 2015 Lifecycle assessment of microalgae to biofuel: Comparison of thermochemical processing pathways *Appl. Energy* **154** 1062–71

[9] Gehrer M, Seyfried H and Staudacher S 2014 Life Cycle Assessment of Btl As Compared To Hvo Paths in Alternative Aviation Fuel Production 1–10

[10] Passell H, Dhaliwal H, Reno M, Wu B, Ben Amotz A, Ivry E, Gay M, Czartoski T, Laurin L and Ayer N 2013 Algae biodiesel life cycle assessment using current commercial data *J. Environ. Manage.* **129** 103–11

[11] Batan L, Quinn J, Bradley T and Willson B 2010 Net Energy and GHG Emissions Evaluation of Biodiesel Derived from Microalgae *Technology* **44** 7975–80

[12] Grierson S, Strezov V and Bengtsson J 2013 Life cycle assessment of a microalgae biomass cultivation, bio-oil extraction and pyrolysis processing regime *Algal Res.* **2** 299–311

[13] Brentner L B, Eckelman M J and Zimmerman J B 2011 Combinatorial life cycle assessment to inform process design of industrial production of algal biodiesel *Environ. Sci. Technol.* **45** 7060–7

[14] Quinn J, de Winter L and Bradley T 2011 Microalgae bulk growth model with application to industrial scale systems *Bioresour. Technol.* **102** 5083–92

[15] Milledge J J and Heaven S 2013 A review of the harvesting of micro-algae for biofuel

production *Rev. Environ. Sci. Biotechnol.* **12** 165–78

[16] Valdez P J, Nelson M C, Wang H Y, Lin X N and Savage P E 2012 Hydrothermal liquefaction of Nannochloropsis sp.: Systematic study of process variables and analysis of the product fractions *Biomass and Bioenergy* **46** 317–31

[17] National Alliance For Advanced Biofuels and Bio-products (NAABB) 2014 Full final report: Section III 1–39,

[18] Richardson J W, Johnson M D, Lacey R, Oyler J and Capareda S 2014 Harvesting and extraction technology contributions to algae biofuels economic viability *Algal Res.* **5** 70–8

[19] Leow S, Witter J R, Vardon D R, Sharma B K, Guest J S and Strathmann T J 2015 Prediction of microalgae hydrothermal liquefaction products from feedstock biochemical composition *Green Chem.* **17** 3584–99

[20] Argonne National Laboratory The Greenhouse gases, Regulated Emissions, and Energy use in Transportation Model *https://greet.es.anl.gov/*

[21] Burnham A, Wang M Q and Wu Y 2006 Development and applications of GREET 2.7 -- The Transportation Vehicle-CycleModel.

[22] Davis, R., Coleman, A., Wigmosta, M., Markham, J., Kinchin, C., Zhu, Y., Jones, S., Han, J., Canter, C., and Li, Q. 2018 2017 Algae Harmonization Study: Evaluating the Potential for Future Algal Biofuel Costs, Sustainability, and Resource Assessment from Harmonized Modeling 1–99

[23] Abodeely J M, Coleman A M, Stevens D M, Ray A E, Cafferty K G and Newby D T 2014 Assessment of algal farm designs using a dynamic modular approach *Algal Res.* **5** 264–73

[24] Zhu Y, Anderson D and Jones S 2018 Algae Farm Cost Model : Considerations for Photobioreactors

[25] Forster, P., V. Ramaswamy, P. Artaxo, T. Berntsen, R. Betts, D.W. Fahey, J. Haywood, J. Lean, D.C. Lowe, G. Myhre, J. Nganga, R. P.; G. Raga M S and R V D Changes in Atmospheric Constituents and in Radiative Forcing. In: Solomon, S. (Ed.), Climate Change 2007: The Physical Science Basic. Contribution of Working Group I to the Fourth Assessment Report of the Intergovernmental Panel on Climate Change; Cambrid

[26] Bare J 2011 TRACI 2.0: The tool for the reduction and assessment of chemical and other environmental impacts 2.0 *Clean Technol. Environ. Policy* **13** 687–96

[27] Environmental Protection Agency Understanding Global Warming Potentials

[28] Wernet G, Bauer C, Steubing B, Reinhard J, Moreno-Ruiz E and Weidema B 2016 The ecoinvent database version 3 *Int. J. Life Cycle Assess.* **21** 1218–30

[29] Al-Sarkal T and Arafat H A 2013 Ultrafiltration versus sedimentation-based pretreatment in Fujairah-1 RO plant: Environmental impact study *Desalination* **317** 55–66

[30] Sengupta M, Xie Y, Lopez A, Habte A, Maclaurin G and Shelby J 2018 The National Solar Radiation Data Base (NSRDB) *Renew. Sustain. Energy Rev.* **89** 51–60

[31] Alexandrov G A and Yamagata Y 2007 A peaked function for modeling temperature dependence of plant productivity *Ecol. Modell.* **200** 189–92

[32] Béchet Q, Laviale M, Arsapin N, Bonnefond H and Bernard O 2017 Modeling the impact of high temperatures on microalgal viability and photosynthetic activity *Biotechnol. Biofuels* **10** 1–11

[33] Sukenik A, Beardall J, Kromkamp J C, Kopecký J, Masojídek J, Van Bergeijk S, Gabai S, Shaham E and Yamshon A 2009 Photosynthetic performance of outdoor Nannochloropsis mass cultures under a wide range of environmental conditions *Aquat. Microb. Ecol.* **56** 297–308

[34] Bae J H 2011 Selection of Suitable Species of of Chlorella, Nannochloris, and Nannochloropsis in High- and Low-Temperature Seasons for Mass Culture of the Rotifer Brachionus plicatilis *Fish Aquat Sci* **14** 323–32

[35] Ras M, Steyer J P and Bernard O 2013 Temperature effect on microalgae: A crucial factor for outdoor production *Rev. Environ. Sci. Biotechnol.* **12** 153–64

[36] Lee A K, Lewis D M and Ashman P J 2013 Harvesting of marine microalgae by electroflocculation: The energetics, plant design, and economics *Appl. Energy* **108** 45–53

[37] Grima E M, Acie F G, Medina A R and Chisti Y 2003 Recovery of microalgal biomass and metabolites: process options and economics **20** 491–515

[38] Pahl S L, Lee A K, Kalaitzidis T, Ashman P J, Sathe S and Lewis D M 2013 Harvesting, Thickening and Dewatering Microalgae Biomass *Algae for Biofuels and Energy* vol 5 (Dordrecht: Springer Netherlands) pp 165–85

[39] Fasaei F, Bitter J H, Slegers P M and van Boxtel A J B 2018 Techno-economic evaluation of microalgae harvesting and dewatering systems *Algal Res.* **31** 347–62

[40] Steel Tubes IN Stainless steel 316 suppliers, *https://www.stindia.com/316-stainless-steel-supplier.html#price*

[41] Shi W, Zhu L, Chen Q, Lu J, Pan G, Hu L and Yi Q 2017 Synergy of flocculation and flotation for microalgae harvesting using aluminium electrolysis *Bioresour. Technol.* **233** 127–33

[42] O'Connell D, Savelski M and Slater C S 2013 Life cycle assessment of dewatering routes for algae derived biodiesel processes *Clean Technol. Environ. Policy* **15** 567–77

[43] Sander K and Murthy G S 2010 Life cycle analysis of algae biodiesel *Int. J. Life Cycle Assess.* **15** 704–14

[44] Hou J, Zhang P, Yuan X and Zheng Y 2011 Life cycle assessment of biodiesel from soybean, jatropha and microalgae in China conditions *Renew. Sustain. Energy Rev.* **15**

5081–91

[45] Cheng M, Rosentrater K A and Wang T 2016 Environmental Impact Analysis of Soybean Oil Production from Expelling, Hexane Extraction and Enzyme Assisted Aqueous Extraction

[46] Sathish A and Sims R C 2012 Biodiesel from mixed culture algae via a wet lipid extraction procedure *Bioresour. Technol.* **118** 643–7

[47] Ramírez-Verduzco L F, Rodríguez-Rodríguez J E and Jaramillo-Jacob A D R 2012 Predicting cetane number, kinematic viscosity, density and higher heating value of biodiesel from its fatty acid methyl ester composition *Fuel* **91** 102–11

[48] Islam M, Magnusson M, Brown R, Ayoko G, Nabi M and Heimann K 2013 Microalgal Species Selection for Biodiesel Production Based on Fuel Properties Derived from Fatty Acid Profiles *Energies* **6** 5676–702

[49] Patil P D, Gude V G, Mannarswamy A, Cooke P, Nirmalakhandan N, Lammers P and Deng S 2012 Comparison of direct transesterification of algal biomass under supercritical methanol and microwave irradiation conditions *Fuel* **97** 822–31

[50] Patil P D, Gude V G, Mannarswamy A, Deng S, Cooke P, Munson-McGee S, Rhodes I, Lammers P and Nirmalakhandan N 2011 Optimization of direct conversion of wet algae to biodiesel under supercritical methanol conditions *Bioresour. Technol.* **102** 118–22

[51] Elliott D C, Hart T R, Schmidt A J, Neuenschwander G G, Rotness L J, Olarte M V., Zacher A H, Albrecht K O, Hallen R T and Holladay J E 2013 Process development for hydrothermal liquefaction of algae feedstocks in a continuous-flow reactor *Algal Res.* **2** 445–54

[52] Jazrawi C, Biller P, Ross A B, Montoya A, Maschmeyer T and Haynes B S 2013 Pilot plant testing of continuous hydrothermal liquefaction of microalgae *Algal Res.* **2** 268–77

[53] Bessette A P 2018 Techno-Economic and Life Cycle Assessment of Hydrothermal Processing of Microalgae for Biofuels and Co-Product Generation

[54] Biddy M, Davis R, Jones S and Zhu Y 2013 Whole Algae Hydrothermal Liquefaction Technology Pathway Whole Algae Hydrothermal Liquefaction Technology Pathway 1–10

[55] Quinn J C, Yates T, Douglas N, Weyer K, Butler J, Bradley T H and Lammers P J 2012 Nannochloropsis production metrics in a scalable outdoor photobioreactor for commercial applications *Bioresour. Technol.* **117** 164–71

[56] Lardon L, Helias A, Sialve B, Steyer J-P and Bernad O 2009 Policy Analysis Life-Cycle Assessment of Biodiesel Production from Microalgae *Environ. Sci. Technol.* **43** 6475–81

[57] Program B 2010 National Algal Biofuels Technology Roadmap *Renew. Energy* 140

[58] Madsen L B, Hoffmann J, Spangsmark D, Deng S, Holm-Nielsen J B, Rosendahl L A, Toor S S and Reddy H 2013 Hydrothermal liquefaction of Spirulina and Nannochloropsis

salina under subcritical and supercritical water conditions *Bioresour. Technol.* **131** 413–9

[59] Bohon M D, Metzger B A, Linak W P, King C J and Roberts W L 2011 Glycerol combustion and emissions *Proc. Combust. Inst.* **33** 2717–24

[60] Huo H, Wang M, Bloyd C and Putsche V 2008 Life-Cycle Assessment of Energy and Greenhouse Gas Effects of Soybean-Derived Biodiesel and Renewable Fuels *Argonne GREET Rep.* 1–101

[61] SIVARAMAKRISHNAN K and RAVIKUMAR P 2011 Determination of Higher Heating Value of Biodiesels *Int. J. Eng. Sci. Technol.* **3** 7981–7

[62] Collet P, Lardon L, Hélias A, Bricout S, Lombaert-Valot I, Perrier B, Lépine O, Steyer J P and Bernard O 2014 Biodiesel from microalgae - Life cycle assessment and recommendations for potential improvements *Renew. Energy* **71** 525–33

[63] Anon, Solar Energy Local; *https://www.solarenergylocal.com*

[64] Asmare A M, Demessie B A and Murthy G S 2013 Theoretical estimation the potential of algal biomass for biofuel production and carbon sequestration in ethiopia *Int. J. Renew. Energy Res.* **3** 560–70

[65] Khanam I A and Deb U K 2016 Calculation of the Average Irradiance and the Microalgae Growth for a Year at CUET, Bangladesh *Am. J. Comput. Math.* **06** 237–44

APPENDIX

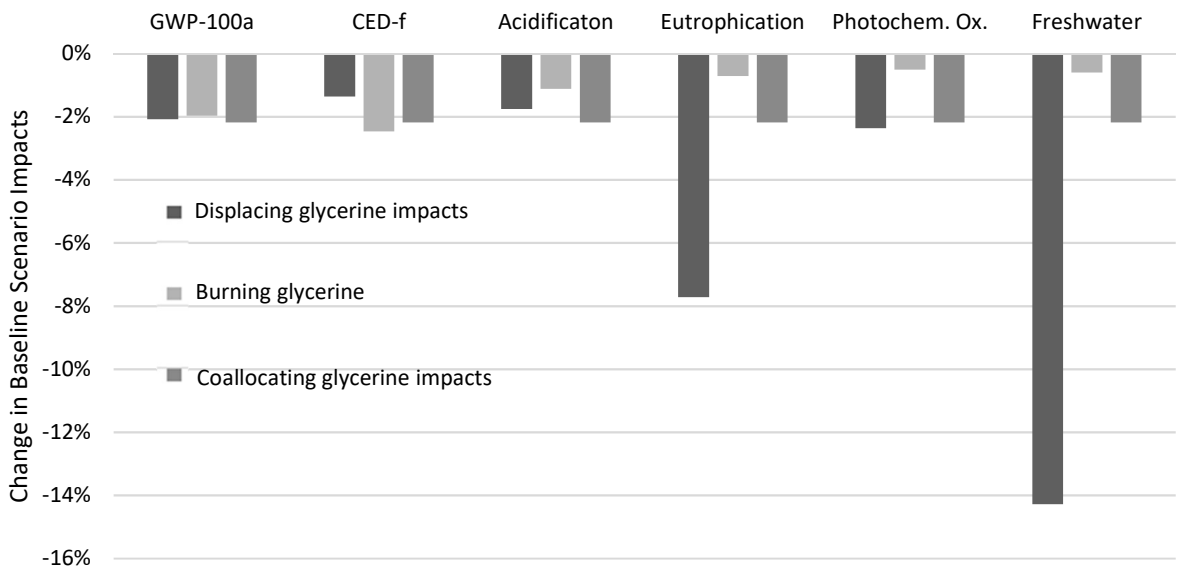

Figure A-1. Change in baseline scenario impacts from the glycerine disregard case by using alternative methods of handling produced glycerine.

Figure A-1, shows the effects of the various methods of handling glycerine impacts discussed in Section 4.4. The 'glycerine disregard case' that each method is compared against simply represents total disregard of glycerine impacts and storage costs. The 'coallocate glycerine impacts' case performs impact allocation based on the market values of the two co-products, i.e. biodiesel and glycerine.

The effects of varying the direct electricity source on freshwater use and photochemical oxidation are illustrated in Figure A-2. Freshwater use does not vary significantly, as fossil and non-fossil electricity contributors of comparable significance to this impact. However, photochemical oxidation does change, as the non-fossil electricity impact (NOx eq./ kWh) is about 94.4% less than that of fossil electricity.

The relative contributions of each process on the total HTL Scenario impact are illustrated in Figure A-3. Hydroprocessing dominates freshwater use contributions as it requires hydrogen, which is assumed produced from water via membrane cell chlor-alkali electrolysis.

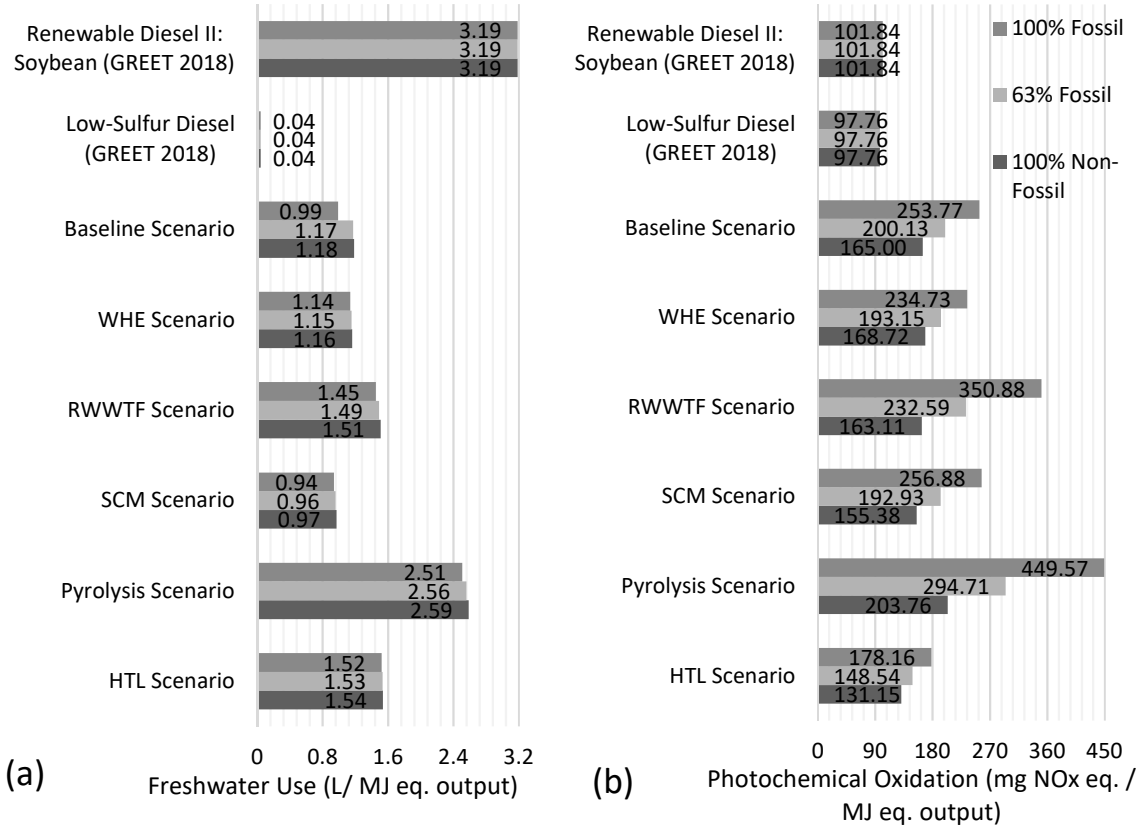

Figure A-2. (a) Freshwater use and (b) photochemical oxidation impacts for the illustrative scenarios using various source mixes for on-site electricity use.

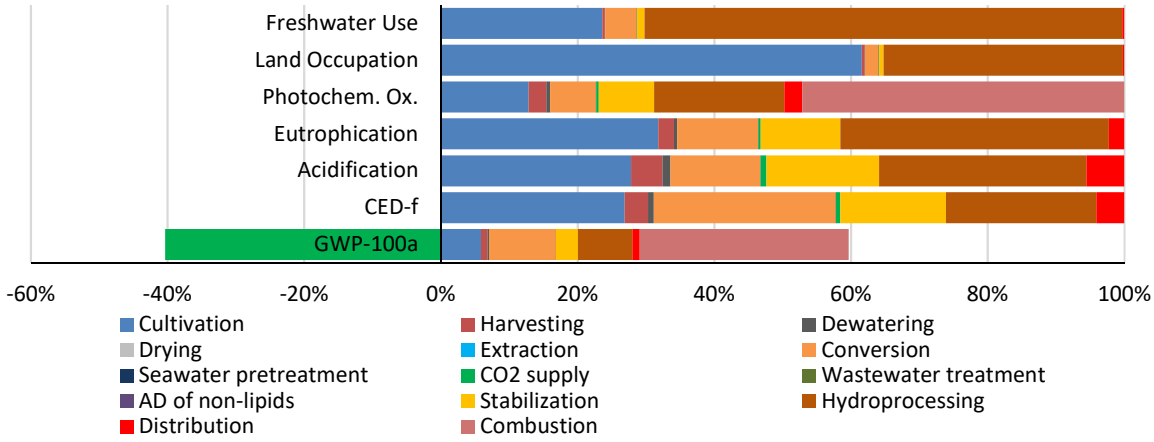

Figure A-3. Process contributions for the HTL Scenario based on 100% fossil-sourced direct electricity use.

Tables A-1 through A-5 enumerate the default values of parameters for process models currently implemented in the framework, as well as the sources for these values (other than for algae harvesting, dewatering, and drying, which are described in Section 3.3). The criteria for the selection of these sources are described in Chapter 2.

Table A-1. Default parameters for the cultivation process model implemented in the framework.

Process model	**Model parameter**	**Value**	**Source**
Flat-Plate PBR	Light saturation level	200 µmol. m^{-2}. s^{-1}	[1]
	Absorption coefficient	.0752 m^2/ g	[1]
	Maximum growth rate	2.5e-2 h^{-1}	[1]
	Maintenance respiration rate	4.32e-4 h^{-1}	[1]
	Biosynthetic efficiency	4 g/ g	[1]
	Optimum temperature	23 ^oC	[1]
	Minimum survivable temperature	5 ^oC	See Section 3.2
	Maximum survivable temperature	40 ^oC	See Section 3.2
	Activation energy	63 kJ/ mol	[1]
	Maximum cell quota of N	0.150 g/ g	[1]
	Minimum cell quota of N	0.010 g/ g	[1]
	Cell quota of N of inocula	0.060 g/ g	[1]
	Half saturation constant for N uptake	0.005 g/ L	[1]
	Maximum specific uptake rate for N	1.5e-6 g. g^{-1}. h	[1]
	Maximum photosynthetic rate	3.6e-2 h^{-1}	[1]
	Photon efficiency	6.5e-7 g/ (µmol of photons)	[1]
	N respiration rate	0 h^{-1}	[1]

Table A-2. Default parameters for the lipid extraction process models implemented in the framework.

Process model	**Model parameter**	**Value**	**Source**
Dry Hexane Extraction	Electricity	0.15465 kWh/ kg_output	[2]
	Heat (non-gas)	2.04 MJ/ kg_output	[2]
	Max recovery rate (lipids)	0.9448	[3]
	Max extraction ratio	1/2.22 kg_lipids/ kg_algae	[2]
	Tap water	0.084 kg/ kg_algae	[2]
	Hexane	0.00382 kg/ kg_output	[2]
Wet Hexane Extraction	Electricity	2.21 kWh/ kg_output	[4]
	Heat (gas)	20.503 MJ/ kg_output	[4]
	Max recovery rate (lipids)	1 (assumption by the paper; superseded by max extraction ratio)	[4]
	Max extraction ratio	1/ 3.53 (kg_lipids/ kg_algae)	[4]
	Unspecified chemical	0.08 kg/ kg_output	[4]
	Wastewater	0.017 m^3/ kg_output	[4]
	Hexane	0.00382 kg/ kg_output	[2]

Table A-3. Default parameters for the fuel conversion processes models implemented in the framework.

Process model	**Model parameter**	**Value**	**Source**
Methyl esterification of dry lipids	Electricity	0.03202 kWh/ kg_oil	[5]
(uses “"esterification of soybean oil || vegetable oil methyl ester || US kg" from Ecoinvent 3.4)	Heat (gas)	0.77812 MJ/ kg_oil	[5]
	Methanol	0.08152 kg/ kg_oil	[5]
	Phosphoric acid	5.69e-4 kg/ kg_oil	[5]
	Sodium hydroxide	8.7152e-4 kg/ kg_oil	[5]
	Citric acid	6.53e-4 kg/ kg_oil	[5]
	Hydrochloric acid	0.0389 kg/ kg_oil	[5]
	Tap water	0.30314 kg/ kg_oil	[5]
	Wastewater	4.3e-5 m^3/ kg_oil	[5]
	Recovery rate	0.88699 kg_FAME/ kg_oil	[5]
Supercritical methanolysis	Electricity	0.413 kWh/ kg_oil	[6][7]
	Heat (gas)	21.662 MJ/ kg_oil	[6][7]
	Methanol depletion	0.08152 kg/ kg_oil	[5]
	Maximum overall conversion efficiency	0.40 kg_FAME/ kg_algae	[6]
	Maximum lipid conversion efficiency	0.84 kg_FAME/ kg_lipids	[6]
Pyrolysis	Electricity	2.31 kWh/ kg_algae	[8]
	Heat (gas)	7.9 MJ/ kg_algae	[8]

Table A-3. (continued)

	HEx efficiency	.85	[8]
	Zeolite	27e-6 kg/ kg_algae	[8]
	Sodium carbonate	0.027 kg/ kg_algae	[8]
	Bio-oil yield	.23 kg/ kg_algae	[6]
	Aqueous phase yield	.20 kg/ kg_algae	[6]
	Biochar yield	0.32 kg/ kg_algae	[6]
	Syngas yield	0.12 kg/ kg_algae	[6]
	Biochar HHV	20 MJ/ kg	[6]
	Syngas HHV	21 MJ/ kg	[6]
Hydrothermal liquefaction	Heat (gas)	6.51 MJ/ kg_algae	
	Max heat recovered	0.61 MJ/ kg_algae	
	HEx efficiency	0.85	
	Sodium carbonate	0.04 kg/ kg_algae	
	HHV of process gases	1.1 MJ/ kg	
	Bio-oil recovery estimation		
	Coefficient L	0.97	[9] (eq. 4)
	Coefficient P	0.42	[9] (eq. 4)
	Coefficient C	0.17	[9] (eq. 4)
	Bio-oil composition estimation		
	Carbon recovered	1 kg_C/ kg_C	[9]
	Nitrogen recovered	0.726 kg_N/ kg_N	[9]
	Hydrogen per carbon	0.145 kg_H / kg_C (assumed)	[9] (Table 2)
	Sulfur per mass bio-oil	0.33 % (assumed from *N. oculata* composition)	[1]

Table A-4. Default parameters for the bio-oil processing process models implemented in the framework.

Process model	**Model parameter**	**Value**	**Source**
Stabilization	Electricity	0.77 MJ/ kg_bio-oil	[8]
	Propane	0.02 kg/ kg_bio-oil	[8]
	Bio-oil recovery rate	0.846	[8]
	Raffine recovery rate	0.154	[8]
Hydroprocessing	Electricity	0.8381 MJ/ kg_stabilized_bio-oil	[8]
	Hydrogen	0.0488 kg/ kg_stabilized_bio-oil	[8]
	Zeolite	4e-4 kg/ kg_stabilized_bio-oil	[8]
	Bio-oil recovery rate	0.823	[10] (mean of 4 cases)

Table A-5. Default parameters for the fuel combustion and distribution process models implemented in the framework.

Fuel Distribution	Electricity	0.34 MJ/ kg_biofuel	[8]
	Recovery rate	0.995	(assumed)
Fuel Combustion[1]			
	CO released	1.335e-3 kg/ kg_biofuel	[11]
	CO_2 released	3.191 kg / kg_biofuel	[11]
	CH_4 released	1.386e-4 kg/ kg_biofuel	[11]
	Total GHGE-100a	3.283 kg/ kg_biofuel	[11]
	NO_x released	32.63e-3 kg/ kg_biofuel	[11]

Table A-5. (continued)

	PM10 released	7.303e-5 kg/ kg_biofuel	[11]
	PM2.5 released	6.742e-5 kg/ kg_biofuel	[11]

[1]Combustion emissions are per mass of Renewable Diesel - II, which has a carbon content of 87.1%; all carbon-based emissions are scaled to the carbon content of the specific algal biofuel.

REFERENCES

(Appendix only)

[1] Quinn J, de Winter L and Bradley T 2011 Microalgae bulk growth model with application to industrial scale systems *Bioresour. Technol.* **102** 5083–92

[2] Hou J, Zhang P, Yuan X and Zheng Y 2011 Life cycle assessment of biodiesel from soybean, jatropha and microalgae in China conditions *Renew. Sustain. Energy Rev.* **15** 5081–91

[3] Cheng M, Rosentrater K A and Wang T 2016 Environmental Impact Analysis of Soybean Oil Production from Expelling, Hexane Extraction and Enzyme Assisted Aqueous Extraction

[4] Gehrer M, Seyfried H and Staudacher S 2014 Life Cycle Assessment of Btl As Compared To Hvo Paths in Alternative Aviation Fuel Production 1–10

[5] Wernet G, Bauer C, Steubing B, Reinhard J, Moreno-Ruiz E and Weidema B 2016 The ecoinvent database version 3 *Int. J. Life Cycle Assess.* **21** 1218–30

[6] National Alliance For Advanced Biofuels and Bio-products (NAABB) 2014 Full final report: Section III 1–39

[7] Brentner L B, Eckelman M J and Zimmerman J B 2011 Combinatorial life cycle assessment to inform process design of industrial production of algal biodiesel *Environ. Sci. Technol.* **45** 7060–7

[8] Bennion E P, Ginosar D M, Moses J, Agblevor F and Quinn J C 2015 Lifecycle assessment of microalgae to biofuel: Comparison of thermochemical processing pathways *Appl. Energy* **154** 1062–71

[9] Leow S, Witter J R, Vardon D R, Sharma B K, Guest J S and Strathmann T J 2015 Prediction of microalgae hydrothermal liquefaction products from feedstock biochemical composition *Green Chem.* **17** 3584–99

[10] Elliott D C, Hart T R, Schmidt A J, Neuenschwander G G, Rotness L J, Olarte M V.,

Zacher A H, Albrecht K O, Hallen R T and Holladay J E 2013 Process development for hydrothermal liquefaction of algae feedstocks in a continuous-flow reactor *Algal Res.* **2** 445–54

[11] Argonne National Laboratory The Greenhouse gases, Regulated Emissions, and Energy use in Transportation Model *https://greet.es.anl.gov/*